Winter 1-31-2022

Strengthening of Long RC Columns Using Near Surface Mounted GFRP Bars

Ahmed Romaih
ahmedromaih@aucegypt.edu

The American University in Cairo

School of Sciences and Engineering

Strengthening of Long RC Columns Using Near Surface Mounted GFRP bars

A Thesis Submitted to

The Department of Construction Engineering

In partial fulfillment of the requirements for the degree of

Master of Science in Construction Engineering

By

Ahmed Hatem Ahmed Romaih

BSc. in Construction Engineering, 2018

The American University in Cairo

Under the Supervision of

Dr. Ezzeldin Yazeed Sayed-Ahmed

Professor and Chairman, The Department of Construction Engineering

Dr. Mohamed Naguib AbouZeid

Professor, The Department of Construction Engineering

August 2021

Dedication

I would like to dedicate this thesis to my father, my mother, my sisters and my fiancée. I thank them for their love, patience, and support.

Acknowledgements

I would like to express my deep gratitude and appreciation to my advisors, Professor Ezzeldin Yazeed and Professor Mohamed AbouZeid, for their patience, guidance, support, and interest in this work, and for the many things I learned from them.

Moreover, I would like to thank Schock Combar for providing the GFRP bars for my thesis in kind.

The experimental work was carried out at the Laboratories of the Department of Construction Engineering in School of Sciences and Engineering, AUC. The help of the technical staff, under the directions of Dr. Omar El-Kadi is greatly appreciated.

The financial support by the AUC is gratefully acknowledged.

Abstract

Many of the existing reinforced concrete (RC) columns are deficient because of numerous reasons such as increase in service loads, deterioration due to environmental attacks, errors in the design and/or construction phase or in the worst case, accidents. These elements require strengthening or repair. Different methods have been developed over the years for solving different rehabilitation problems. Recently, advanced composites used for external bonding in the form of fabrics or laminates have become an accepted method. The use of Fibre-Reinforced Polymers (FRPs) in this process is a promising technology, especially that these materials are corrosion-free. One of the new techniques used for strengthening is placing Near-Surface Mounted (NSM) FRP bars in the existing structural elements.

The aim of this research is to examine the effectiveness of strengthening reinforced concrete (RC) columns using NSM glass fibre reinforced polymer (GFRP) bars. Seventeen columns with a cross-section of 250 × 250 mm will be cast and tested under the effect of axial loads and uniaxial bending. The test parameters include different slenderness ratios as well as the length and diameter of the NSM GFRP bars.

The results are interpreted to analyze the effectiveness of using NSM GFRP bars in strengthening RC columns and to test whether they can be used as efficiently as steel/concrete jackets or CFRP sheets. The performance of the strengthened columns are evaluated based on the measured load-deflection curves, the ultimate observed strength, and the crack width and spacing at estimated service load.

The experimental investigation proved that NSM GFRP bars can be effectively used to strengthen RC columns as GFRP bars have an advantage over CFRP due to low cost relative to CFRP. It is lighter, has a higher resistance to corrosion, and has a higher tensile strength with an ease of use relative to steel plates. It is also maintenance free, meaning that there will be no rehabilitation cost.

Keywords: Near surface mounted, RC columns, GFRP, strengthening

Table of Contents

List of Tables

List of Figures

List of Symbols

A_v	:	area of the stirrups
c	:	cover of longitudinal steel reinforcement
E_{sc}	:	modulus of elasticity of concrete
E_s	:	modulus of elasticity of steel reinforcement
E_F	:	modulus of elasticity of CFRP
$f_ç$	:	28 days concrete cylinder compressive strength
f_{yt}	:	yield strength of the stirrups
f_u	:	ultimate strength of steel reinforcement
f_y	:	Yield strength of steel reinforcement
f'_c	:	compressive strength of concrete cylinder
f'_{cu}	:	compressive strength of concrete cube

Chapter 1: Introduction

1.1 Background

Concrete structures form the majority of buildings all over the world and especially in Egypt. They have the advantage of taking many different shapes. In addition to its unique aesthetics achieved in construction, concrete offers other advantages such as its relative cheaper cost when compared to steel structures. Moreover, it does not require labor as skilled as those in the steel structure field. However, concrete structural elements may require strengthening for various reasons, for example, changing functions, corrosion to the reinforcement that require repair and other natural effects, mistakes in construction or in the design processes, and so forth.

Concrete is a material that is good in undergoing compression, however, weak in tension, therefore, it can carry almost the whole compressive force in columns but steel reinforcement is needed to carry the tension from flexural loading. However, steel can easily corrode and as such RC members frequently need strengthening. Fibre reinforced polymers (FRPs), which were recently developed, are great materials in strengthening concrete elements due to their lightweight, resistance to corrosion, high tensile strength and many other factors that will be described hereunder.

Flexural as well as shearing strength of the structural elements should be increased to accomplish the necessary strength and to sustain the ductile mode of failure given by flexural behavior. For the situation where the concrete does not meet the predefined compressive strength, for instance, the shear limit is affected more than the flexural limit, hence, increasing the transverse reinforcement in needed.

There are many strengthening techniques that are available to the designer giving him different options to choose from based on the different cases at hand. Most of the examples in the literature shows the use of steel plates/jackets to strengthen the columns or carbon fibre reinforced polymers (CFRP) sheets/ bars. The aim of this thesis is to study the flexural performance of long columns strengthened with near surface mounted (NSM) glass fibre reinforced polymers (GFRP) bars using different alignments under different cases of loading.

1.2 Problem Statement

As mentioned above, FRP materials are easier to apply than steel reinforcement, relatively lighter and can be transported at a lower cost and most importantly they are not exposed to corrosion. However, FRP and especially carbon fibre reinforced polymers CFRP are more expensive than steel reinforcement, but GFRP's come at a relatively low cost that is not much more expensive than steel reinforcement. However, not many studies have been made on the effect of strengthening columns with FRPs and therefore they are rarely used in the strengthening and repair market worldwide.

GFRP needs to be tested for their ability to increase the strength of eccentrically loaded columns. Many studies have been done on strengthening flexural members (beams and slabs) using FRP laminates and bars; results showed that FRP increases the flexural ability of structural elements. However, strengthening columns subject to flexure and axial load using FRP (and particularly NSM) bars still needs to be investigated.

1.3 Methodology

Long columns with different slenderness ratios will be examined experimentally to investigate the effect of strengthening them using NSM GFRP bar with different diameters. Seventeen column with a 250 × 250 mm cross-section are tested. The columns heights range between 1.5 m to 2.5 m.

Of each height, two columns are tested as the control samples (no NSM GFRP bars) and two columns are strengthened using one no. 8 NSM GFRP bar in the tension side. The remaining two samples for the 1.5m and 2.0m columns are strengthened with one no. 12 NSM GFRP bar and only one sample of the 2.5m columns will be strengthened with one no. 12 NSM GFRP bar.

1.4 Objectives and Thesis Outline

This study consists mainly of an experimental investigation. Thesis includes a report on the results of this experimental program which is carried out on seventeen full scale reinforced concrete columns that are strengthened using various NSM GFRP bars.

The experimental investigation is performed mainly to check the effect of strengthening long RC columns using NSM GFRP bars. Effect of GFRP bar diameters as well as column slenderness are also scrutinized. The thesis presents the failure modes and cracking patterns recorded during the experimental work for the different tested columns.

The thesis consists of five chapters. The background is presented in the first chapter which is the introduction chapter to the thesis. The literature review is given in Chapter two. Chapter three presents the experimental program. The results are presented, analyzed and discussed in Chapter four. The summary and conclusions of the present study are given in Chapter five.

The main objective of this study is to assess the strengthening process of long RC columns using near surface mounted glass fibre reinforced polymer bars.

Chapter 2: Literature Review

Over the years, the addition of steel plates on concrete flexural elements was used to repair and strengthen damaged members. Even with the potential of an effective and relatively cheap solution, some major problems may be stumbled upon with corrosion, orientation and placement of the steel plates as well as bonding. Steel plate bonding has therefore never gained great acceptance by consultants and professionals.

Using fibre Reinforced Polymers (FRP) for the repair and strengthening of concrete members has gained universal acceptance as an advanced method for the retrofitting and improvement of existing concrete structures. Fibre Reinforced Polymers have many advantages over traditional strengthening techniques, which is the use of steel bars or plates, due to its resistance to corrosion, ease of installation, its high strength to weight ratio, and the improved durability of the composite material.

Performance of reinforced concrete members that have been reinforced using fibre reinforced polymers has been studied by Catbas (1997). He reported that shear failure will have the higher probability of occurring if CFRP sheets were applied to the tension side. This result was also found in other methods of flexural strengthening. This shows the shift of the failure from flexural ductile, to shear brittle. Therefore, the members require shear strengthening as well as flexural to provide a similar increase in the shear strength to achieve the desired mode of failure (Catbas, 1997).

Innovative composite materials such as FRP have been used in the repair of reinforced structures and has been a success in the construction industry since the 1950's according to Rubinsky (1954). RC structures can advance from the high modulus and specific strength, durability, lightweight and resistance to corrosion and carbonation of the FRP, and from the ease of installation which means cost and time saving.

After the failure of other repair methods due to problems such as bonding and corrosion, the interest in FRP increased. The use of FRP elements increased in the 1980's when they were used in cases where the concrete was subject to severe chemical attacks according to (ACI 440R-96).

Commonly used fibres in strengthening and repair include glass, carbon and aramid. The ones preferred in the construction industry are glass and carbon fibres. Carbon fibres are harder and stronger than glass fibres, however, they are much more expensive (ACI 440R-96).

The construction industry is interested in FRP reinforcement as it does not have the durability issues related to steel reinforcement such as corrosion. Using FRP in concrete members has the following advantages: high strength and elasticity, resistance to corrosion, durability, lightweight, chemical resistance, impact resistance and electro-magnetic permeability.

2.1 Physical and Mechanical Properties of FRP

The following must be taken into consideration before discussing the properties of FRP bars. FRP is an anisotropic material, meaning that the longitudinal axis is the strong axis. Moreover, unlike steel, properties of FRP change from one type to another. Volume, type of fibre, fibre orientation, dimensional effects, surface condition and quality control during manufacture have a major effect on the product characteristics. Furthermore, like all materials, the mechanical properties are affected by factors such as the duration of loading, temperature and moisture.

2.1.1 Specific Weight

Due to their much lighter weight than steel, fibre reinforced polymers have a specific weight ranging from 1.5 to 2.0 gm/cm^3. The light weight has many advantages such as decreased storage and transportation costs and faster installation on site due to the ease of handling by the skilled labor when compared to steel reinforcement.

2.1.2 Tensile Strength

Fibre reinforced polymer bars reach the ultimate tensile strength without showing any material yielding. All mechanical properties of FRP are measured in the strong direction, which is the longitudinal direction. As seen in Figure 2.1 below, GFRP is a brittle material. When the bar fails, the fibres deflect in all directions like a brush.

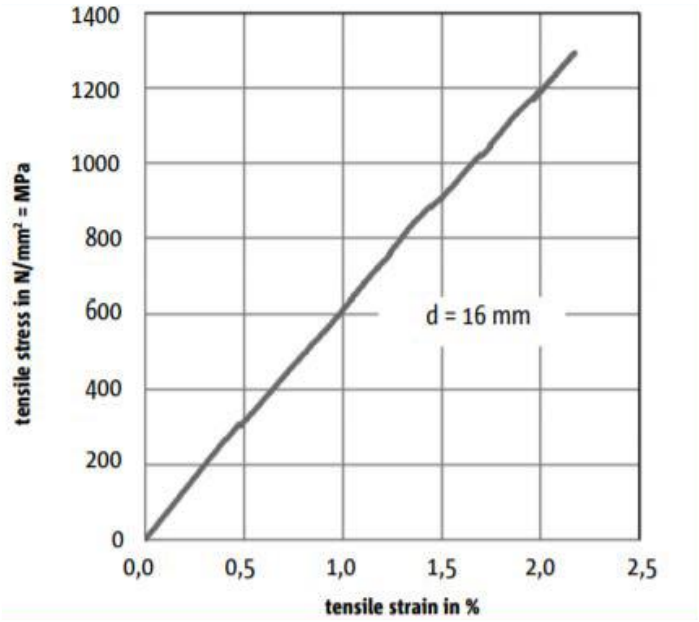

Figure 2.1 Stress Strain Curve of a 16mm bar (Schock Combar, 2015)

The tensile strength of FRP materials is a function of the diameter of the bar, which is unlike steel. Fibres located at the center of the bar cross section are not exposed to the same stresses as the fibres at the outer surface of the bar due to shear lag, (Faza, 1991). The result of this is a reduced strength in bars with a larger diameter. As an example, GFRP bars produced by one U.S. manufacturer have a tensile strength ranging from nearly 480 MPa for No. 9 (28.7 mm) bars to 890 MPa for No. 3 (9.5 mm) bars, (Ehsani, 1993).

2.1.3 Shear Strength

Generally, composites have a very low shear strength. For example, FRP bars can be cut very easily in the perpendicular direction to the longitudinal axis with saws. This defect can be overcome in most cases by orienting the FRP bars such that they will resist the applied loads through axial tension.

2.1.4 Fatigue Resistance

Studies have shown that FRP bars display good fatigue resistance. Most of the research that has been published in regards to fatigue resistance have been studying high-modulus fibres such as carbon and aramid. The fibres were exposed to many

cycles of tension-tension loading different applications such as aerospace. Tests that had 10 million cycles of loading showed that carbon epoxy composites had better fatigue strength than steel. However, glass polymers had a lower fatigue strength than steel at low stress ratio, Schwarz, (1992).

Other researchers, Porter (1993) showed that glass fibre bars showed good in shear when subjected to 10 million cycles. Franke, (1991) studied glass fibre bars in prestressing applications where the bars were subjected to repeated cyclic loading with a maximum stress of 496 MPa and a stress range of 345 MPa. The bars could stand more than 4 million cycles of loading before failure initiated at the anchorage zone

FRP materials are relatively expensive, and while laminates are commercially available in the Middle East and many countries, rods are still not readily available and can be brought only by special orders. NSM conventional steel reinforcement bars can be considered a possible alternative to NSM rods because it is commercially available, it costs only a fraction of the cost of the FRP rods, and because it could provide a solution to the low bond resistance of some types of FRP rods. The concern with corrosion of such bars can be eliminated using various methods such as insulation of the limited areas when NSM bars are applied. In addition, bars can be easily given a U shape, and its use increases the development of the NSM bars on the bottom side.

2.2 NSM Technique

The NSM technique has proven to be a successful with the conventional steel reinforcing bars in bending moment regions in slabs and beams. The NSM method has an advantage over FRP laminates as FRP laminates may be subjected to the harsh effects of finishing and wear and tear. The use of NSM FRP as reinforcement is shown by the increased interest to understand its bonding properties to concrete, De Lorenzis, (2004).

Recent researches have been studying the use of NSM FRP rods, De Lorenzis and Nanni, (2001). The shortened explanation of this method is that Grooves are cut into the surface of an existing concrete member to a specified depth and width (e.g. 25 mm by 25 mm) along the length of the bar to be used. The epoxy resin is then used to

fill about half of the groove. The FRP bar is then placed into the epoxy in the groove and is pressed lightly. The groove is then filled with epoxy and the surface is leveled, De Lorenzis and Nanni, (2001).

Coelho (2015) explains the steps for applying NSM fibre reinforced polymers (FRP) as follows:

1. Making the groove on the external surface of the structure to be strengthened
2. Cleaning the grooves using an air/water jet to ensure that there are no loose parts and no remains that will inhibit the bonding
3. Preparing the FRP to be used
4. Preparing the adhesive/epoxy to be used as per the technical specifications
5. Filling the groove with the adhesive
6. Placing the FRP in the groove while applying light pressure to ensure that the adhesive covers the whole surface area of the FRP and the groove. This step requires special care to make sure that there are not any voids/air bubbles.
7. Removing any excess adhesive and leveling the surface.

NSM FRP strengthening has the following advantages over externally bonded reinforcement, (Coelho, 2015):

1. Reduced preparation time
2. Less susceptible to debonding due to a larger bonding surface area
3. More protection of the FRP against wear and tear and acts of vandalism
4. Less visual impact

2.3 Experimental Results for FRP Flexural Strengthening

NSM strengthening technique is particularly used in the tension side of reinforced concrete members. Externally Bonded Reinforcement (EBR) is subjected to harsh environmental and mechanical conditions besides wear and tear that can cause severe damage to the reinforcement, Hassan, (2004). Therefore, NSM FRP can be used as an alternative to EBR because the bars will not be exposed to external factors. Blaschko and Zilch (1999) showed the effect of using NSM CFRP strips that were

placed into grooves cut into the surface of concrete members. The results showed that the NSM strips had a larger anchorage capacity than externally bonded strips.

Si Youcef et al. (2015) show that the orientation in which the FRPs are applied to a reinforced concrete (RC) column affects its strength. For example, if carbon fibre sheets are wrapped transversally around the RC column, then the concrete strength will increase due to the confinement effect that increased the buckling resistance of the longitudinal bars. However, if a column is strengthened with longitudinal FRPs then the result would be an increase in the flexural strength of the column.

Rahai, A. and Akbarpour, H. (2017) Studied the effect of strengthening columns with a high slenderness ($\frac{kl}{r} = 29$), with different orientations of CFRP sheets. The orientations included transverse reinforcement, longitudinal reinforcement and reinforcement oriented at an angle of 45 degrees. The columns were tested under repeated eccentric compression. The results showed that the transversally strengthened column had an increased load bearing capacity of 14%, 76% for the column strengthened with longitudinal fibres and 52% for the column strengthened with fibres oriented at 45 degrees. They concluded that all strengthening methods resulted in an increase in the compressive and bonding stiffness of the columns.

Moreover, Kheyroddin A. and Kargaran A. (2019), tested the effect of strengthening short columns that are exposed to axial loads as well as cyclic lateral loads. After wrapping the columns with FRP, the mode of failure changed from shear to flexural. Moreover, the results showed an increase in ductility as well as a 128% increase in load capacity experimentally as well as an analytical increase of 137%.

Large scale prestressed concrete members were tested by Hassan and Rizkalla (2002) to investigate the feasibility of different FRP materials used to increase the flexural strength of concrete members using different strengthening methods. The results showed that the NSM bars are cost effective and feasible for the strengthening of concrete members.

According to the ACI 440.1R-01, the following expression is used to determine the development length, L_d, to avoid splitting failures in FRP reinforced concrete members.

$$L_d = 0.028 \frac{\pi d^2 f_u}{4\sqrt{f'_c}} \qquad 2.1$$

Where, f'_c is the compressive strength of concrete after 28 days, f_u is the tensile strength and d is the bar diameter. Research done by Hassan and Rizkalla, (2004), concluded that the ACI equation is not suitable for NSM FRP bars strengthening techniques due to major discrepancies in the results for the following reasons:

- The ACI expression only covers the bond of FRP to concrete. However, NSM bars mainly depend on the characteristics of the adhesive used to bond the bars to the member. The adhesive is usually much smoother than concrete and hence requires a longer development length to reach the same bonding strength as that of concrete (Hassan and Rizkalla, 2004).

- The expression assumes that the coefficient of friction between the FRP bar and concrete is 1.0. This coefficient of friction is applicable for the bonding of steel bars and concrete and has been confirmed in many research. However, FRP bars and adhesives such as epoxy have a much lower coefficient of friction that ranges between 30-60% of that in the ACI expression. This also includes that NSM FRP bars require a longer development length. (Hassan and Rizkalla, 2004)

- The ACI expression assumes that the FRP bar is confined by stirrups, which is not the case in NSM FRP bars and therefore a longer development length is required. (Hassan and Rizkalla, 2004)

Chapter 3 - Experimental Program

This chapter goes through the details of the test specimens, testing setup and procedures. Seventeen full-scale column specimens were tested to obtain detailed information about the behavior of reinforced concrete columns strengthened using near-surface mounted glass fibre-reinforced polymer bars (NSM-GFRP). The detailed results of the tested columns are presented in Chapter 4.

3.1 Specimen Details

The test program was designed to study the effects of various factors that affect the behavior of columns, namely: type of NSM reinforcement (GFRP Rebar), bar size (8mm and 12mm), column slenderness (columns 1.5m, 2.0m and 2.5m long).

Table 3.1 lists and summarizes the dimensions and configuration of the columns. Six columns with a height of 1.5m, six columns with a height of 2.0 m and five columns with a height of 2.5m are tested. Two specimens of each height were not strengthened to act as control specimens and were designed to fail in flexure. The remaining specimens were strengthened with various configurations and types of NSM GFRP bars, with the objective of increasing the capacity and changing failure towards a flexural mode. Two of the specimens of each height were strengthened with NSM GFRP bars with a diameter of 8mm. The bar covered the whole length of the 1.5m and the 2.0m columns. However, only 2.0m were covered with the NSM GFRP bars for the 2.5m long column as the length of the bar is only 2.0m. The remaining two specimens for the 1.5m and 2.0m columns were strengthened with NSM GFRP bars with a diameter of 12mm that covered the whole length of the columns. Only one specimen was strengthened with a 12mm NSM GFRP bar in the 2.5m column that only covered 2.0m of the length of the column.

The names of the specimens were determined based on their height, and then followed by a letter (C) that stands for column and then two numbers: (00) is a control specimen, (08) is a column that is strengthened with one no.8 GFRP bar and (12) is a column strengthened with one no.12 bar. The sample name is then followed by a number (either 1 or 2) indicating whether this is the first or the second sample to be

tested. For example sample 2.0-C08-1 is a 2.0m high column strengthened with an 8mm diameter GFRP bar and is the first column of the series.

Table 3.1 Specimen details and strengthening information

Specimen ID	Length (m)	Steel stirrups	Longit. Rft.	GFRP bar dia. (mm)	GFRP bar Length (m)	$\lambda = \frac{kl}{r}$	μ_{GFRP}
1.5-C00-1	1.5	no.8 at 150 mm	8no.12	-	-	12	0
1.5-C00-2	1.5	no.8 at 150 mm	8no.12	-	-	12	0
1.5-C08-1	1.5	no.8 at 150 mm	8no.12	8	1.5	12	0.0008
1.5-C08-2	1.5	no.8 at 150 mm	8no.12	8	1.5	12	0.0008
1.5-C12-1	1.5	no.8 at 150 mm	8no.12	12	1.5	12	0.0018
1.5-C12-2	1.5	no.8 at 150 mm	8no.12	12	1.5	12	0.0018
2-C00-1	2.0	no.8 at 150 mm	8no.12	-	-	16	0
2-C00-2	2.0	no.8 at 150 mm	8no.12	-	-	16	0
2-C08-1	2.0	no.8 at 150 mm	8no.12	8	2	16	0.0008
2-C08-2	2.0	no.8 at 150 mm	8no.12	8	2	16	0.0008
2-C12-1	2.0	no.8 at 150 mm	8no.12	12	2	16	0.0018
2-C12-2	2.0	no.8 at 150 mm	8no.12	12	2	16	0.0018

Specimen ID	Length (m)	Steel stirrups	Longit. Rft.	GFRP bar dia. (mm)	GFRP bar Length (m)	$\lambda = \frac{kl}{r}$	μ_{GFRP}
2.5-C00-1	2.5	no.8 at 150 mm	8no.12	-	-	20	0
2.5-C00-2	2.5	no.8 at 150 mm	8no.12	-	-	20	0
2.5-C08-1	2.5	no.8 at 150 mm	8no.12	8	2	20	0.0008
2.5-C08-2	2.5	no.8 at 150 mm	8no.12	8	2	20	0.0008
2.5-C12-1	2.5	no.8 at 150 mm	8no.12	12	2	20	0.0018

3.1.1 1.5m Columns

Figure 3.1 shows the dimensions and details of the six 1.5m long column specimens, before strengthening them with the NSM GFRP bars. The columns have a height of 1.5 meters, a cross section with dimensions 250×250mm, and they have a tapered increased cross-section reaching 250×500mm at the top, as they were tested using a point loading arrangement with a 250mm eccentricity. Figure 3.1 also shows the reinforcement elevation of the six 1.5m long column specimens, before strengthening with (GFRP). All six columns have longitudinal and shear reinforcement. Figure 3.2 shows the details of the reinforcement.

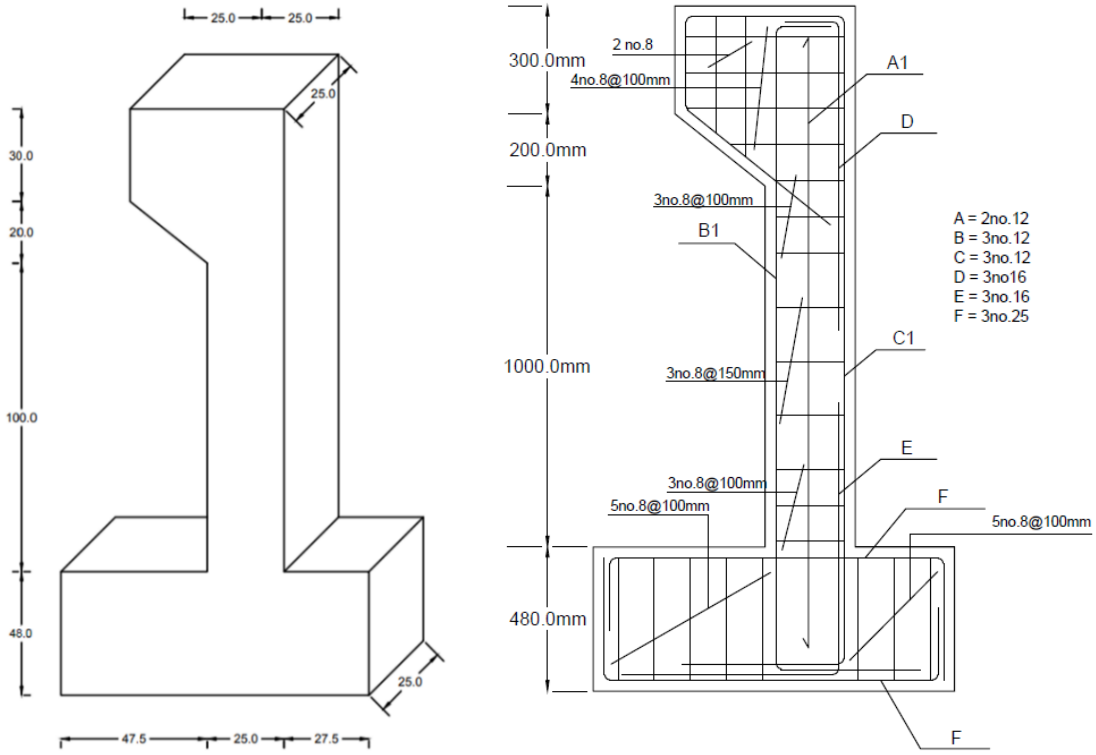

Figure 3.1 General view and cross section of the (1.5m) RC Column specimen

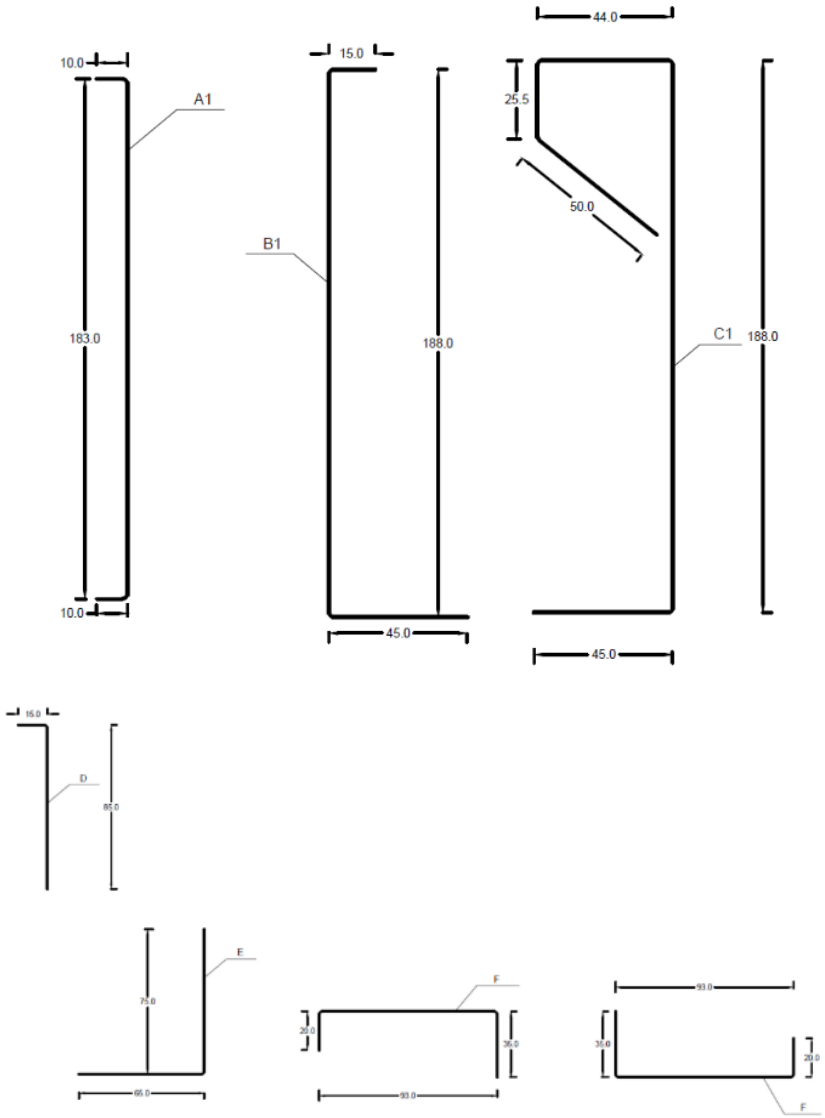

Figure 3.2 Cross Section in all (1.5m) column before strengthening

3.1.2 2.0m Column

Figure 3.3 shows the dimensions and details of the six 2.0m long column specimens, before strengthening with the NSM GFRP bars. The columns have a height of 2.0 meters, a cross section with dimension 250×250mm, and they have a tapered increased cross-section reaching 500×500mm at the top, as they were tested using a point loading arrangement with a 250mm eccentricity. Figure 3.3 also, shows the reinforcement elevation of the six 2.0m column specimens, before strengthening with NSM GFRP. All six columns contained longitudinal and shear reinforcement. Figure 3.4 show the details of the reinforcement.

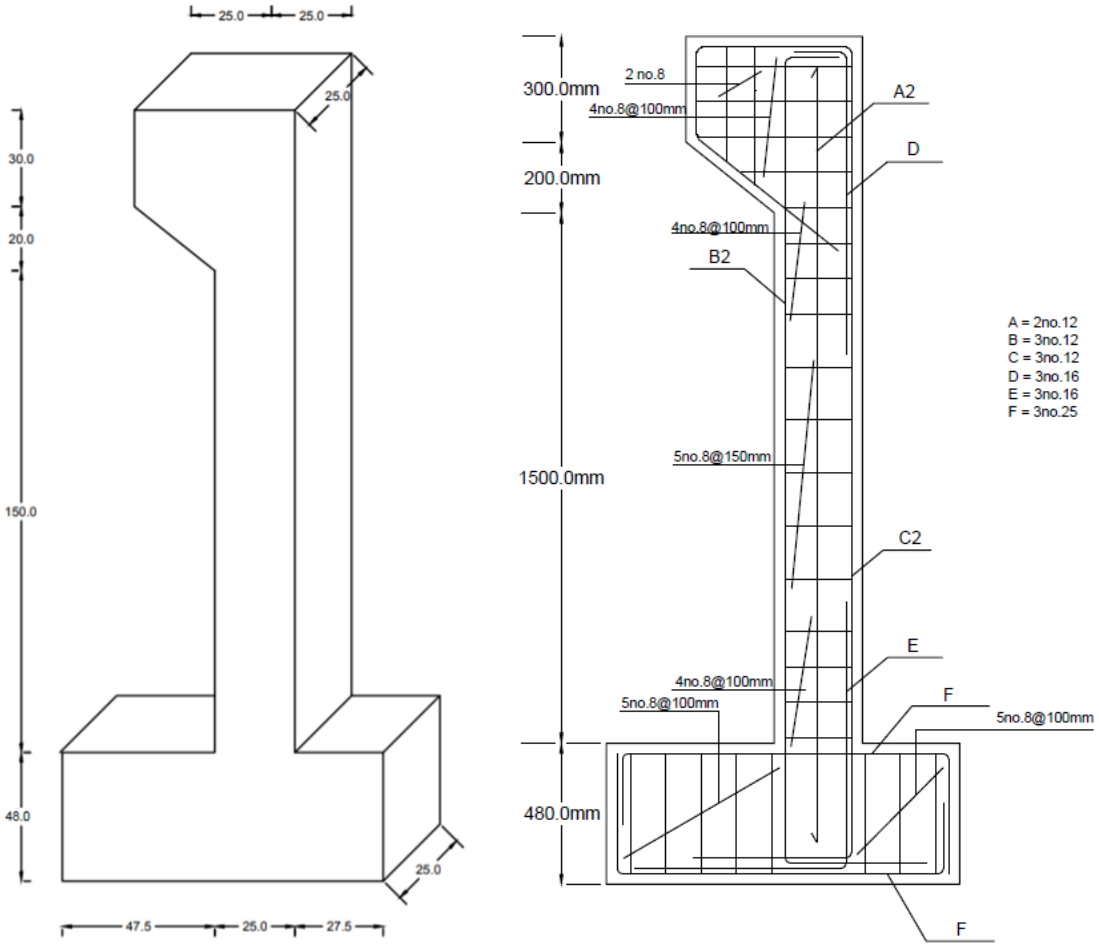

Figure 3.3 General view of the (2.0m) RC Column specimen

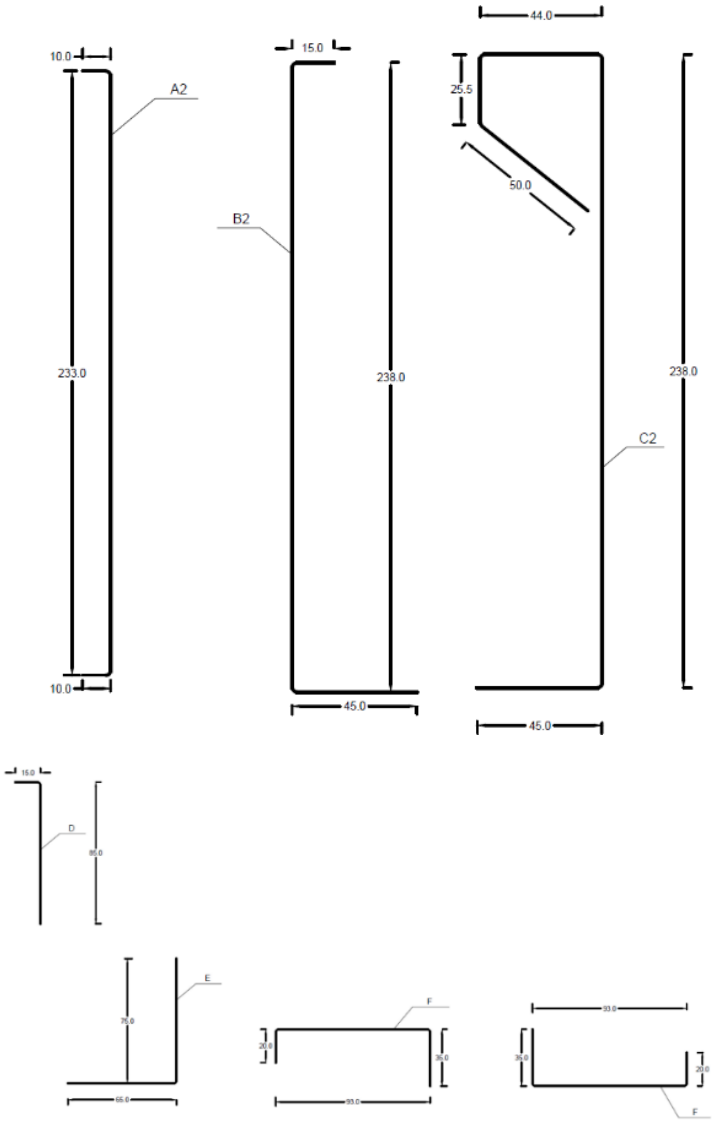

Figure 3.4 Steel layout in all (2.0m) columns before strengthening

3.1.3 2.5m Column

Figure 3.5 shows the dimensions and details of the five 2.5m long column specimens, before strengthening with the NSM GFRP bars. The columns have a height of 2.5 meters, a cross section with dimension 250×250mm, and they have a tapered increased cross-section reaching 500×500mm at the top, as they were tested using a point loading arrangement with a 250mm eccentricity. Figure 3.5 also, shows the reinforcement elevation of the five 2.5m column specimens, before strengthening with NSM GFRP. All six columns contained longitudinal and shear reinforcement. Figure 3.6 shows the details of the reinforcement.

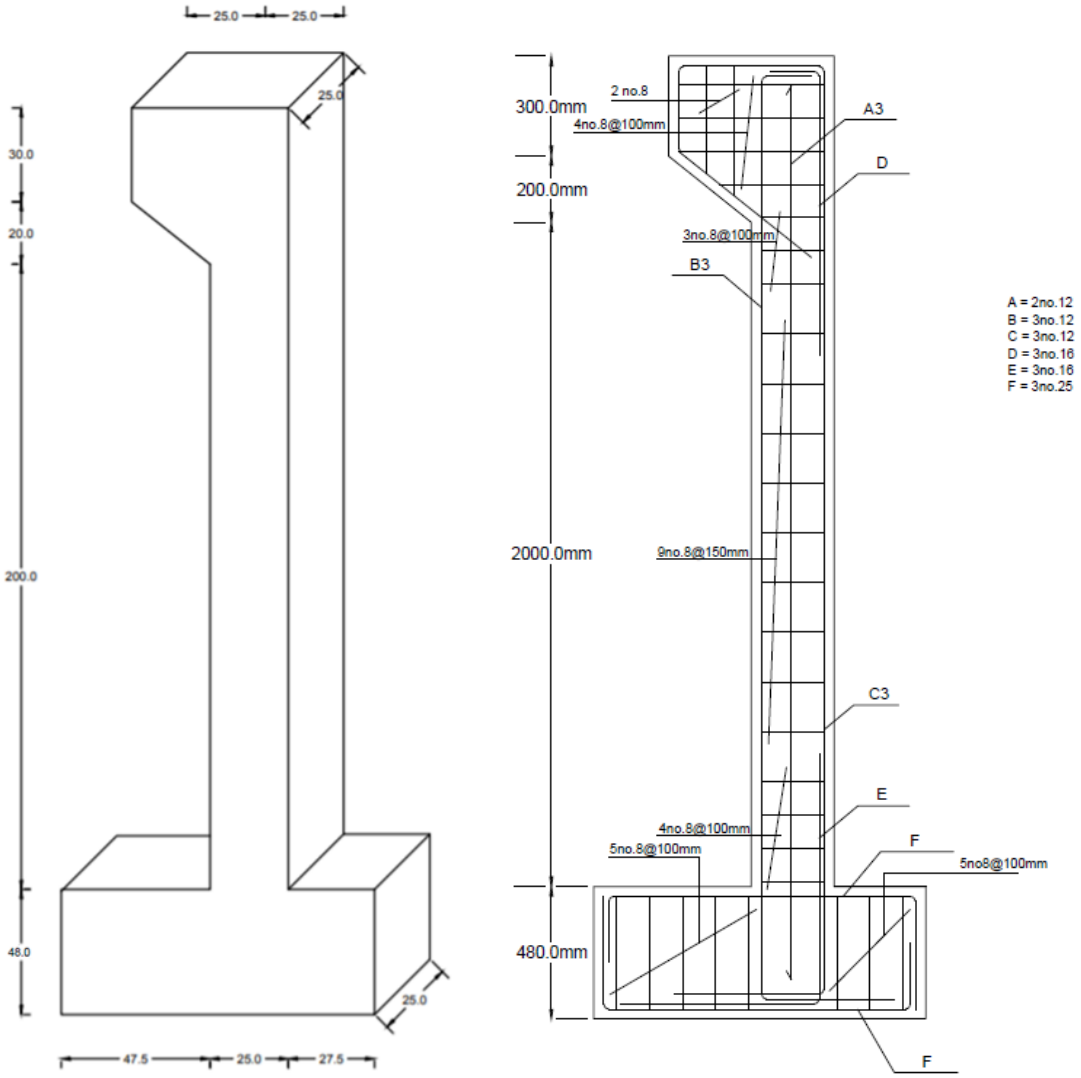

Figure 3.5 General view of the (2.5m) RC Column specimen

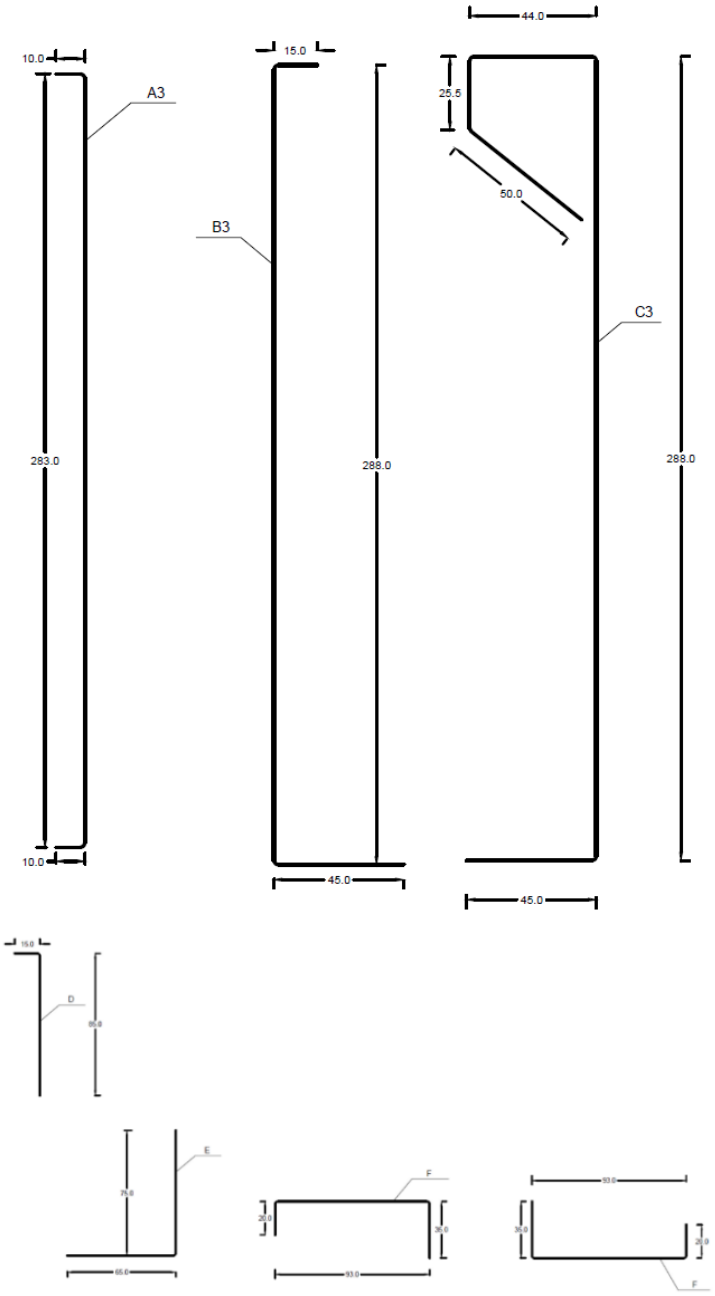

Figure 3.6 Steel layout in all (2.5m) columns before strengthening

The main reinforcement in the critical section was 8no.12 steel bars and the effective depth was 211 mm. In determining the maximum capacity, the compression zone is entirely within the compression side of the column, and the longitudinal reinforcement ratio calculated to be about 1.45%, which is a practical value. The transverse reinforcement was two legged no.8 mm spaced at 150 mm. This corresponds to about 1.88 times the minimum transverse reinforcement required by the 2005 ACI

code (ACI, 2005) for 30 MPa target concrete strength. This level of reinforcement was selected because it is commonly used in actual columns.

Two columns from each size were not strengthened to act as control specimens. The remaining columns were strengthened with NSM GFRP bars. Two columns from each size were strengthened with one no.8mm GFRP bar in the tension side. Two columns from the 1.5m and 2m and 1 column from the 2.5m were strengthened with one no.12mm GFRP bar in the tension side. Hence, three test results were reported from each column size.

3.2 Specimen Strengthening

3.2.1 Control Specimens 1.5-C00

Specimens 1.5-C00-1 and 1.5-C00-2 are the control columns, and hence are not strengthened with NSM GFRP reinforcement. The control specimens are tested to yield the results of strengthened columns to be compared later to NSM GFRP strengthened ones.

3.2.2 Specimens 1.5C-08

These specimens were cast just like the control specimen. The grooves were made during casting with a cross section of 25×25mm. An 8 mm diameter bar was then added in the tension side with a length of 1.5m to cover the whole length of the column and the grooves were then filled with epoxy resin. These columns give information on the efficiency of using base strengthening compared to the control column.

3.2.3 Specimens 1.5-C12

These specimens were cast just like the control specimen. The grooves were made during casting with a cross section of 250×250mm. A no.12 mm bar was then added in the tension side with a length of 1.5m to cover the whole length of the column and the grooves were then filled with epoxy resin. These columns give information on the efficiency of using base strengthening compared to the control column. Comparing

the results of 1.5-C08 will show the advantages of the increasing the area of the NSM GFRP bars used.

3.2.4 Control Specimens 2.0-C00

Specimens 2.0-C00-1 and 2.0C00-2 are the control columns, and hence are not strengthened with NSM GFRP reinforcement. The control specimens are tested to yield the results of strengthened columns to be compared later to NSM GFRP strengthened columns. The increased column height will consider effect of the slenderness (kL/r = 16) and how the increased secondary moment affects the load that the column can withstand.

3.2.5 Specimens 2.0-C08

The specimens were cast just like the control specimen. The grooves were made during casting with a cross section of 25×25mm. A no.8 mm bar was then added in the tension side with a length of 2.0m to cover the whole length of the column and the grooves were filled with epoxy resin. This column gives information on the efficiency of using base strengthening compared to the control column. The increased column height will show the effect of the slenderness (kL/r = 16) and how the increased secondary moment affects the load that the long column can withstand. The result of the added NSM GFRP bar will be reported to see the increased load that the column can withstand.

3.2.6 Specimens 2.0-C12

The specimens were cast just like the control specimen. The grooves were made during casting with a cross section of 25×25mm. A no.12 mm bar was then added in the tension side with a length of 2.0m to cover the whole length of the column and the grooves were filled with epoxy resin. This column gives information on the efficiency of using base strengthening compared to the control column. The increased column height will show the effect of the slenderness (kL/r = 16) and how the increased secondary moment affects the load that the long column can withstand. The result of the increased area of NSM GFRP reinforcement used will be compared to the no.8 mm

bar to see the effect of GFRP strengthening on columns. The aim is to see how much more stresses the column can withstand with the added GFRP.

3.2.7 Control Specimens 2.5-C00

Specimens 2.5-C00-1 and 2.5-C00-2 are the control columns, and hence are not strengthened with NSM GFRP reinforcement. The control specimens are tested to yield the results of strengthened columns to be compared later to NSM GFRP strengthened ones.

The increased column height will show the effect of column's slenderness as long column now has a kl/r ratio of 20 and how the increased secondary moment affects the load that the column can withstand.

3.2.8 Specimens 2.5-C08

These specimens were cast just like the control specimen. The grooves were made during casting with a cross section of 25×25mm. A no.8 mm bar was then added in the tension side with a length of 2.0m and the grooves were filled with epoxy resin. This column gives information on the efficiency of using base strengthening compared to the control column. The increased column height will show the effect of the eccentric load on the long column now that the column has a buckling length (kl/r) of 20, and how the increased moment affects the load that the column can withstand. The result of the added NSM GFRP bar will be reported to see the increased load that the column can withstand.

3.2.9 Specimens 2.5-C12

These specimens were cast just like the control specimen. The grooves were made during casting with a cross section of 25×25mm. A no. 12 mm bar was then added in the tension side with a length of 2.0m and the remaining were filled with epoxy resin. This column gives information on the efficiency of using base strengthening compared to the control column. The increased column height will show the effect of the eccentric load on the long column now that the column has a buckling length (kl/r) of 20, and how the increased moment affects the load that the column can withstand. The result of

the added NSM GFRP bar will be reported to see the increased load that the column can withstand. The result of the increased area of NSM GFRP reinforcement used will be compared to the no.8 mm bar to see the effect of GFRP strengthening on columns. The aim is to see how much more stresses the column can withstand with the added GFRP.

3.3 Materials Properties

3.3.1 Concrete

All the concrete used was ready mixed and was supplied by the El-Sewedy Ready-mix Company with the same specifications, to ensure uniformity of the concrete used. All samples were casted on the same day from the same ready-mix truck. The slump of the concrete was adjusted before casting to the required value by adding super-plasticizer.

With the cast, twelve standard cubes (150 mm × 150 mm× 150 mm) were prepared and cast in metal forms. The cubes were cured and tested at 28 days according to ASTM standards and tested on the same day when the columns were tested to obtain a value of the compressive strength on that day. Table 3.2 gives the properties of concrete. The twelve cubes were tested on two days and therefore two averages for the six cubes that were tested on the test day f_{cu} are shown in the table. The 28-days cube strength was higher than the target strength.

Table 3.2 Compressive strength of concrete on day of testing of column specimens

Sample	Peak Load (kN)	f_{cu} (MPa)
1	895.9	39.8
2	714.7	31.8

Sample	Peak Load (kN)	f_{cu} (MPa)
3	839.6	37.3
4	970	43.1
5	878.7	39.1
6	805	35.8
7	868.7	38.6
8	1046	46.5
9	986.8	43.9
10	1005.5	44.7
11	887	39.4
Average	**899.8**	**40 ± 8.2**

3.3.2 Reinforcing Steel bars

Table 3.3 summarizes the properties of all types of conventional reinforcing steel used in the column specimens.

Table 3.3 Reinforcing Bars Properties

Reinforcement Type	Bar Size	Area* (mm^2)	F_y (MPa)	E_s (GPa)
Longitudinal	no. 12	113	454	203

Reinforcement Type	Bar Size	Area* (mm^2)	F_y (MPa)	E_s (GPa)
Longitudinal	no. 16	201	424	203
Transverse (Stirrups)	no. 10	79	436	204

*Calculated from nominal diameter

3.3.3 GFRP Bars

Type GFRP deformed rods with no.8 mm and no.12 mm nominal diameter were used. Figure 3.8 shows the surface of a typical rod. The tensile strength (f_{Fcs}) and tensile modulus of elasticity (E_F) of the GFRP rods were determined from the manufacturer and reported to be 1900 MPa and 124 GPa, respectively. As seen from the graph in Figure 3.7, the GFRP bar has a higher stress for the same strain when compared to the steel reinforcement.

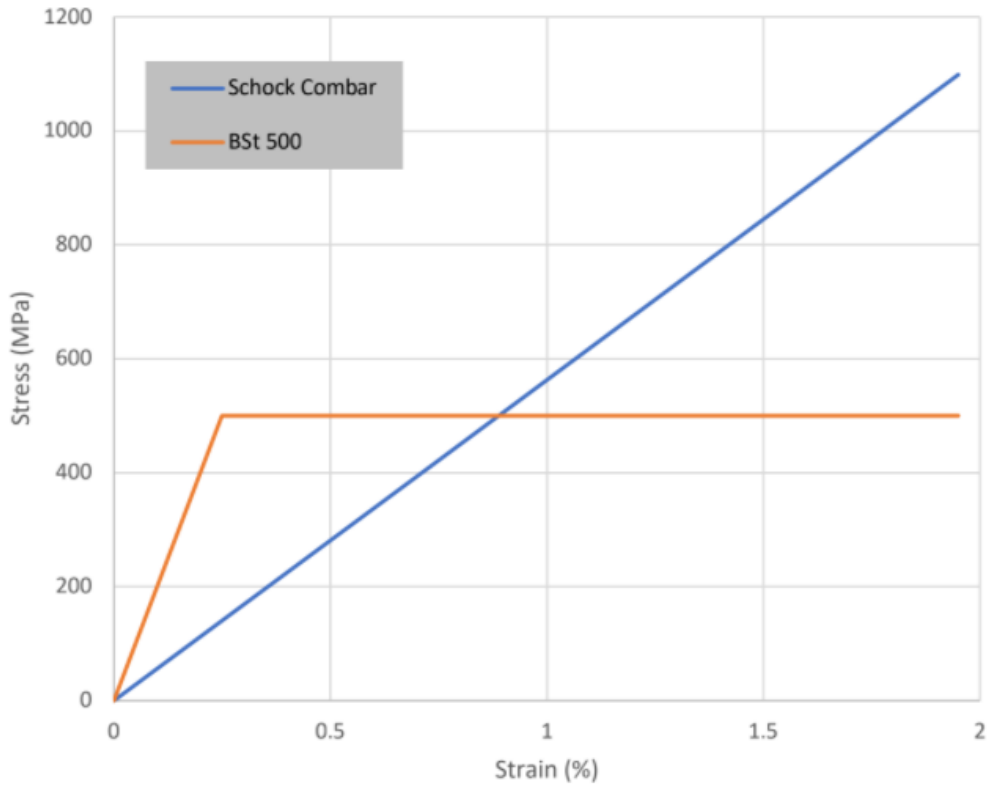

Figure 3.7 Stress-Strain Graph of GFRP Bar (Schoeck ComBAR, 2018)

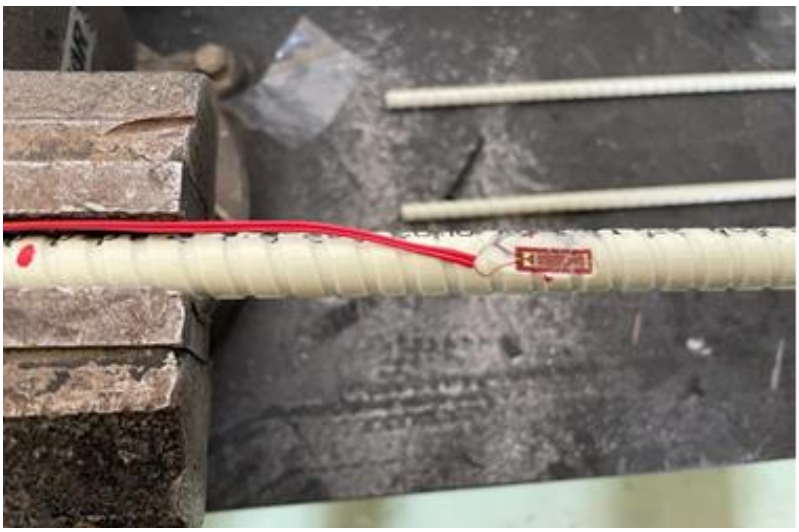

Figure 3.8 Surface configuration of no. 8 mm Type GFRP rod

3.3.4 Epoxy Resin

The epoxy resin used (CMB Kemapoxy 165) to bond the NSM strengthening GFRP rods is manufactured locally in Egypt by CMB Company. It was designed for use on vertical and overhead surfaces, and its mechanical properties, as specified by the manufacturer, compressive strength is higher than 78 MPa as shown in Figure 3.9, and Flexural strength in excess 39 MPa (ASTM D 695 &ASTM D 790).

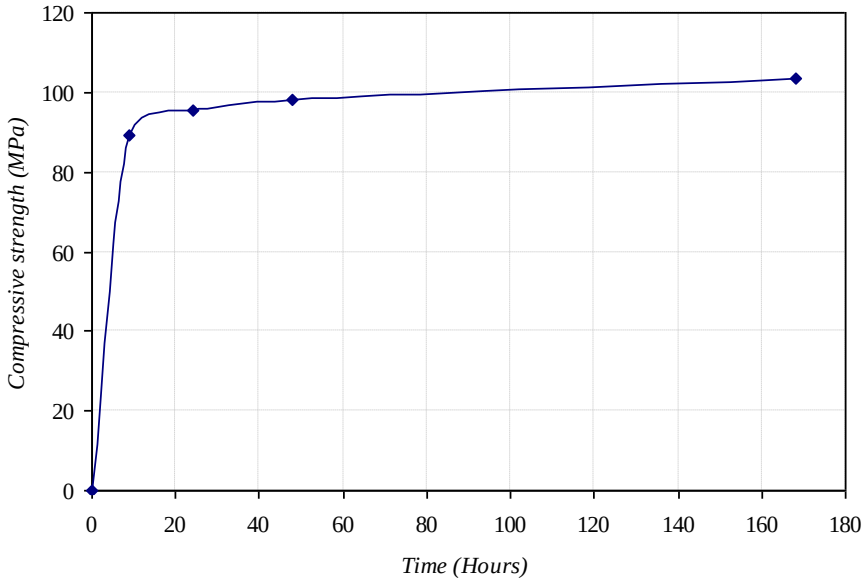

Figure 3.9 Compressive strength of Epoxy Resin (MPa) (CMB International, 2021)

3.4 Casting of the Specimen

Figure 3.10 and Figure 3.11 show a general view of the column steel reinforcement ready in the formwork. The concrete cover outside the stirrups was ensured by placing plastic spacers between the stirrups and the wooden forms. The forms were oiled one day before casting.

Figure 3.10 Steel reinforcement placed in the formwork

Figure 3.11 Column specimens after strengthening the formwork and adding the stain gauges ready for concrete casting

Figure 3.12 shows the locations of the strain gauges attached to bars of specimens for all columns. The strains in the longitudinal bars in the tension zones were monitored by two strain gauges.

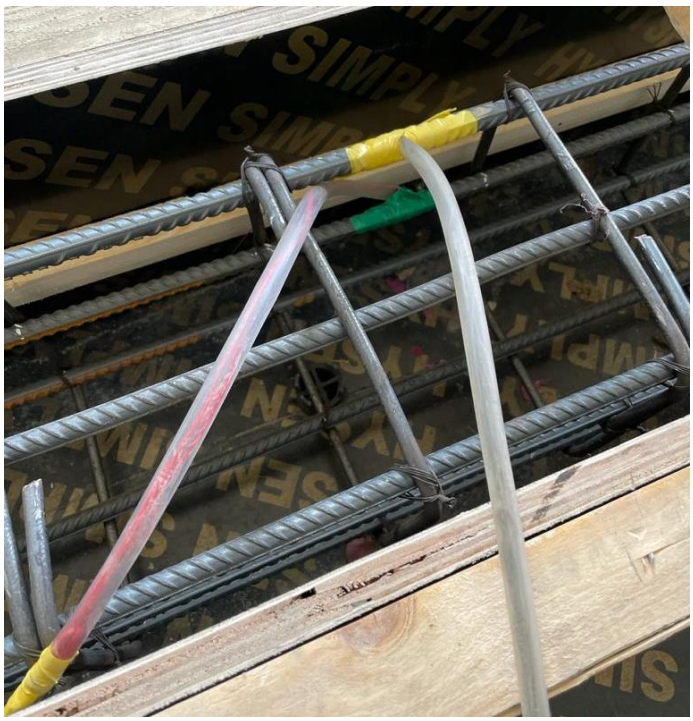

Figure 3.12 Location of strain gauge attached to steel bars of specimens

The concrete was placed slowly and in two layers, as shown in Figure 3.13, to allow proper vibration. The surface of the concrete was finished half an hour after casting was completed. The concrete cubes were cured to test with the column specimens. Unlike the columns, the concrete cubes were not vibrated, but compacted by the standard Roding procedure.

Figure 3.13 Casting the concrete

3.5 Strengthening Techniques

Figure 3.15 shows the steps taken to strengthen the columns using NSM reinforcement. In all specimens the grooves were formed before casting. The size of the groove was 25 × 25 mm to allow for clearance around the rod or bar for proper bond as shown in Figure 3.16 and in the schematic plan in Figure 3.14.

The strain gauges were attached to the GFRP bars as shown in Figure 3.17. The groove was then filled half depth with epoxy paste, the strengthening reinforcement was placed in the groove and lightly pressed. This ensured good contact area between the epoxy and the reinforcement. The groove was then filled with more paste and the surface is leveled a shown in Figure 3.18. The epoxy was allowed to cure for more than 96 hours before testing was started in all strengthened specimens.

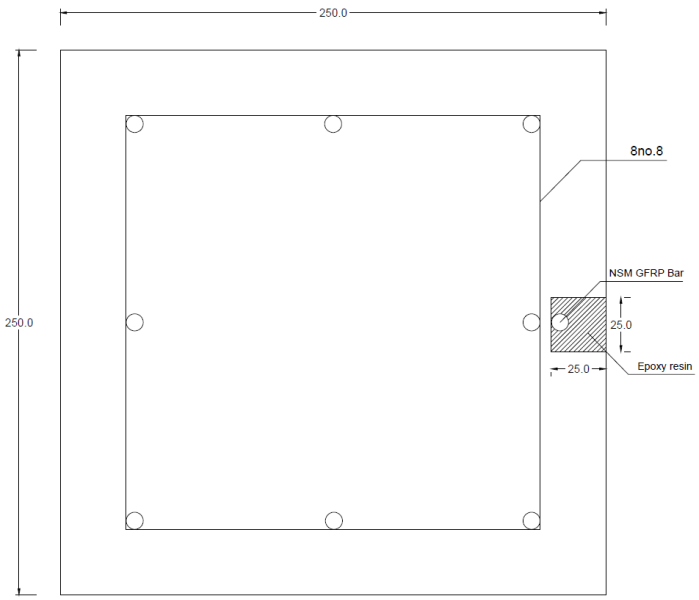

Figure 3.14 Schematic Drawing of the (NSM-GFRP) bar in the column cross section

Figure 3.15 Grooves set during formwork

Figure 3.16 GFRP bars placed in grooves

Figure 3.17 Strain Gauges attached to GFRP Rods

Figure 3.18 GFRP rods covered with epoxy resin

3.6 Test Set-up and Instrumentation

As shown in Figure 3.19, the columns were held from both sides by 2 customized Z-shaped steel sections to have a fixed support and stop any movements to the footing.

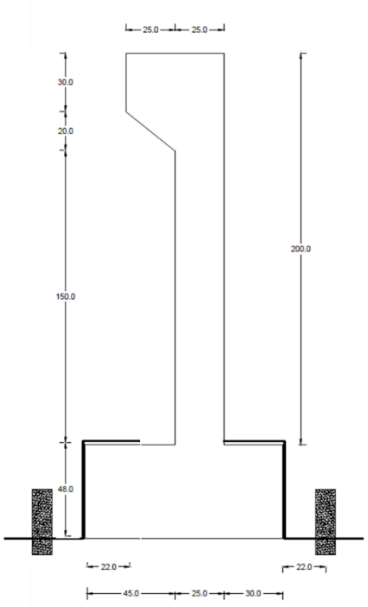

Figure 3.19 Test Setup of the columns

The columns were loaded under a point loading as shown in Figure 3.20 with an eccentricity of 25cm. A steel head was customized to cover the column head and distribute the point load over the whole area.

The vertical deflection was measured horizontally and vertically by placing 2 LVDTs at the column head in Figure 3.21.

Figure 3.20 General View of the Test Set-up for Column 1.5mG8(1)

Figure 3.21 General View of the Test Set-up for Column 1.5mG8(1)

A large number of surface strain reading was necessary to learn about the pattern of flow of the forces through the test region. Electrical resistance strain gauges were used to measure the strains in the main steel reinforcement bars, the concrete surface and the GFRP bar at critical locations of the test region. The gauges were attached to the bars, and then protected with waterproofing material, wax, and vinyl tape. The presence of the tape de-bonded a part of the bar (about 35 mm) from the concrete.

Chapter 4 – Results and Discussion

Chapter 3 described a test program which was designed to gain more information about the behavior of reinforced concrete columns strengthened using NSM GFRP rods. This chapter describes the results of the experimental program.

4.1 Methodology for Evaluating Results

The columns were strengthened to improve their capacity and their overall behavior. Hence evaluating the improvement is based on comparing the increase in load capacity, the change in mode of failure (MOF), as well as the improvement in cracking pattern and in control of crack width at service load. Four strain gauges were used to analyze the results; one strain gauge on the concrete, one on the NSM GFRP bar and two on the steel reinforcement in the middle of the column height (maximum tension) as shown in Figure 4.1.

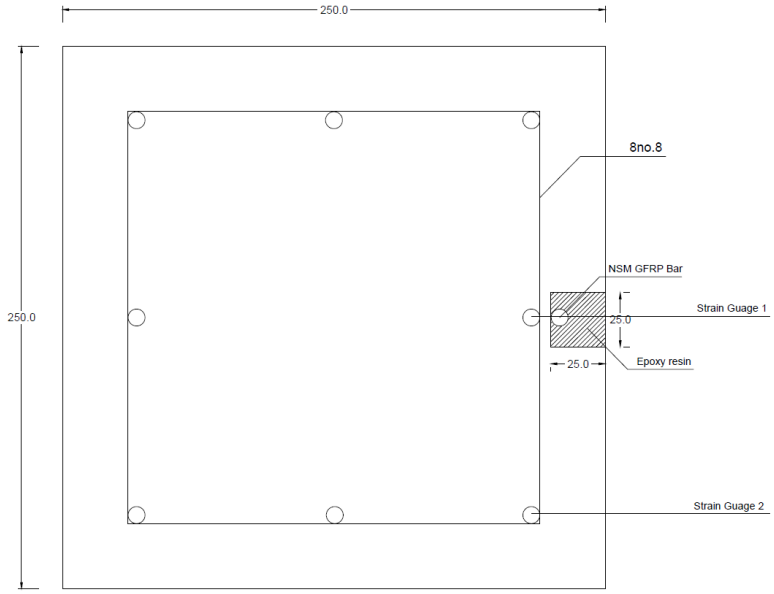

Figure 4.1 Location of the 2 steel strain gauges

4.2 Results

4.2.1 Samples 1.5-C00

These two columns are not strengthened with NSM GFRP bars. They act as control specimen to be enable comparing their results to the strengthened columns and know the effects of adding the NSM GFRP bars and the improvements obtained by strengthening. For the first column, cracks were formed in the middle of the column in the tension side as shown in Figure 4.2. The cracks propagated into deeper cracks as the load increased, one crack widened and propagated until failure took place at a load of 430 kN. A typical flexural failure was formed. Figure 4.3 shows that the LVDTs showed a maximum horizontal deflection of 18mm and maximum vertical deflection of 0.37mm in the column head. For the second control column, the LVDTs showed a maximum horizontal deflection of 19mm and maximum vertical deflection of 0.23mm in the column head. All strain gauges failed in the second column.

Figure 4.2 Cracks at the Tension Side of Column 1.5C00

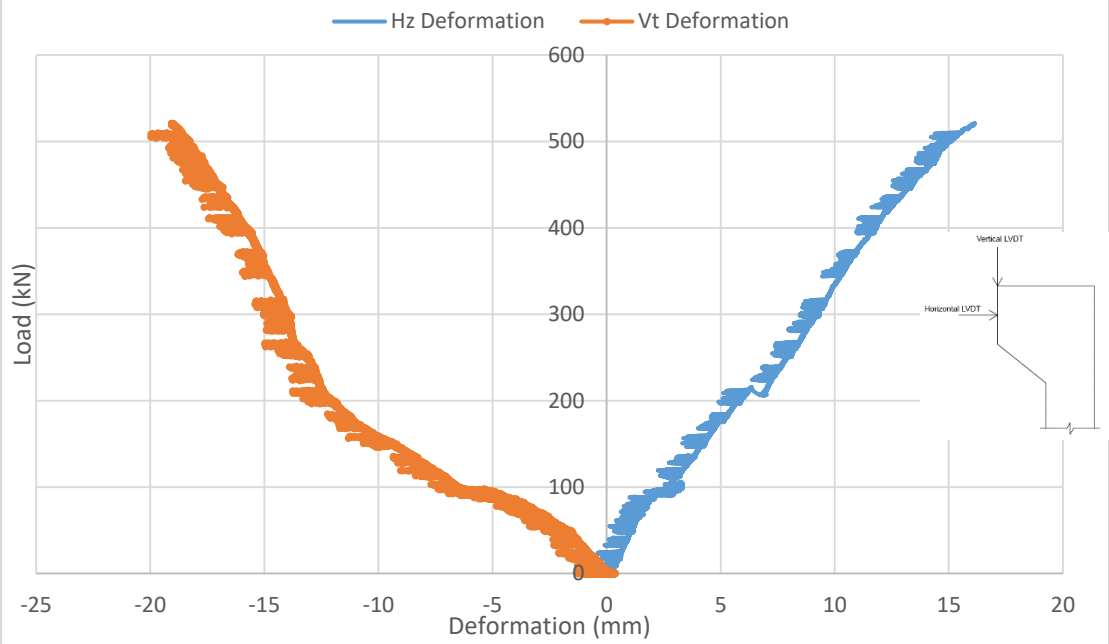

Figure 4.3 Sample 1.5-C00-1 Load-Deformation Graph

Figure 4.4 shows the load strain graph of the column. It shows that the column cracking load is 100 kN with a failure load of 430 kN, with a steel yielding strain equal to 0.0022. There were no results for the other control sample as all strain gauges failed.

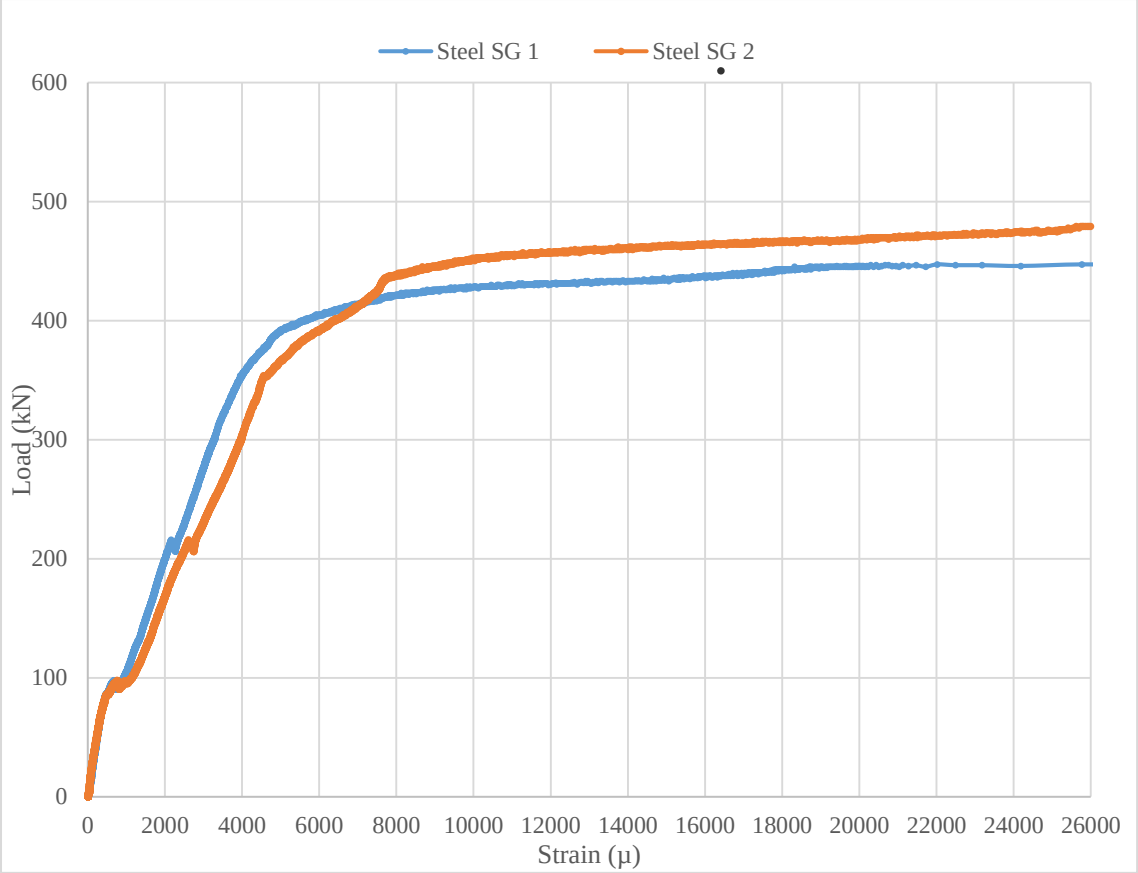

Figure 4.4 Sample 1.5-C00 Load-Strain Graph

4.2.2 Samples 1.5-C08

These two columns are strengthened with one NSM GFRP bar with a diameter of 8mm in the tension side of the column. They will be compared to the control samples to know the effects of GFRP bars, and the improvements obtained by strengthening. For the first column, Cracks were formed in the middle of the column in the tension side at 520kN for the first column and 530kN for the second column as shown in Figure 4.5 and Figure 4.6 respectively. The cracks propagated into deeper cracks as the load increased, one crack widened and propagated until failure took place. The average failure load for this series is 525kN. A typical flexural failure was formed. For the first column, Figure 4.7, the LVDTs showed a maximum horizontal deflection of 17.8mm and maximum vertical deflection of 0.56mm in the column head. For the second column, Figure 4.8, the LVDTs showed a maximum horizontal deflection of 17.6mm and a maximum vertical deflection of 0.35mm.

Figure 4.5 Cracks at the tension side of Column 1.5-C08-01

Figure 4.6 Cracks at the tension side of Column 1.5-C08-2

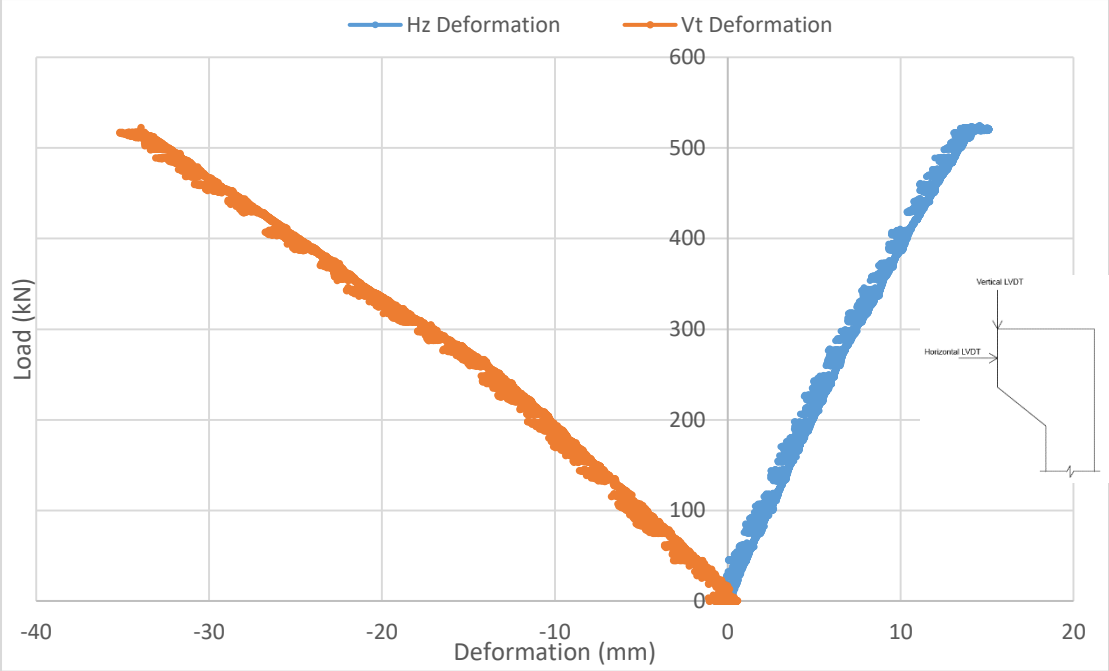

Figure 4.7 Sample 1.5-C08-1 Load-Deformation Graph

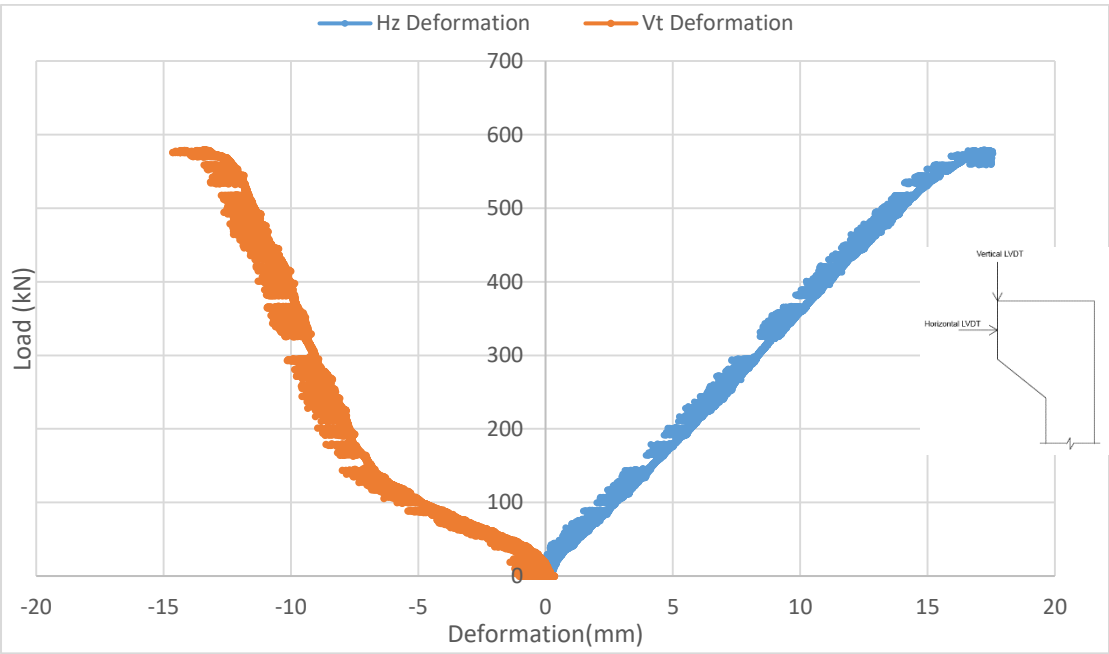

Figure 4.8 Sample 1.5-C08-2 Load-Deformation Graph

Figure 4.9 shows the load strain graph of the first column. It shows that the column cracking load is 100 kN. The failure load is 520 kN, with a steel yielding strain equal to 0.0021. The GFRP strain gauge failed in this specimen. Figure 4.10 shows the

load strain graph of the second column. It shows that the column cracking load is 100 kN, the failure load is 530 kN with a steel yielding strain equal to 0.0019. The GFRP strain at failure load is 0.005. The load-strain graphs show that there was a jump in the strain at the failure load. This is because as the load increases the column deformation increases, hence increasing the eccentricity/second order effect on the columns. This causes the cracks to propagate and widen and therefore the stiffness of the column decreases. Thus, a jump in the strain is expected to occur.

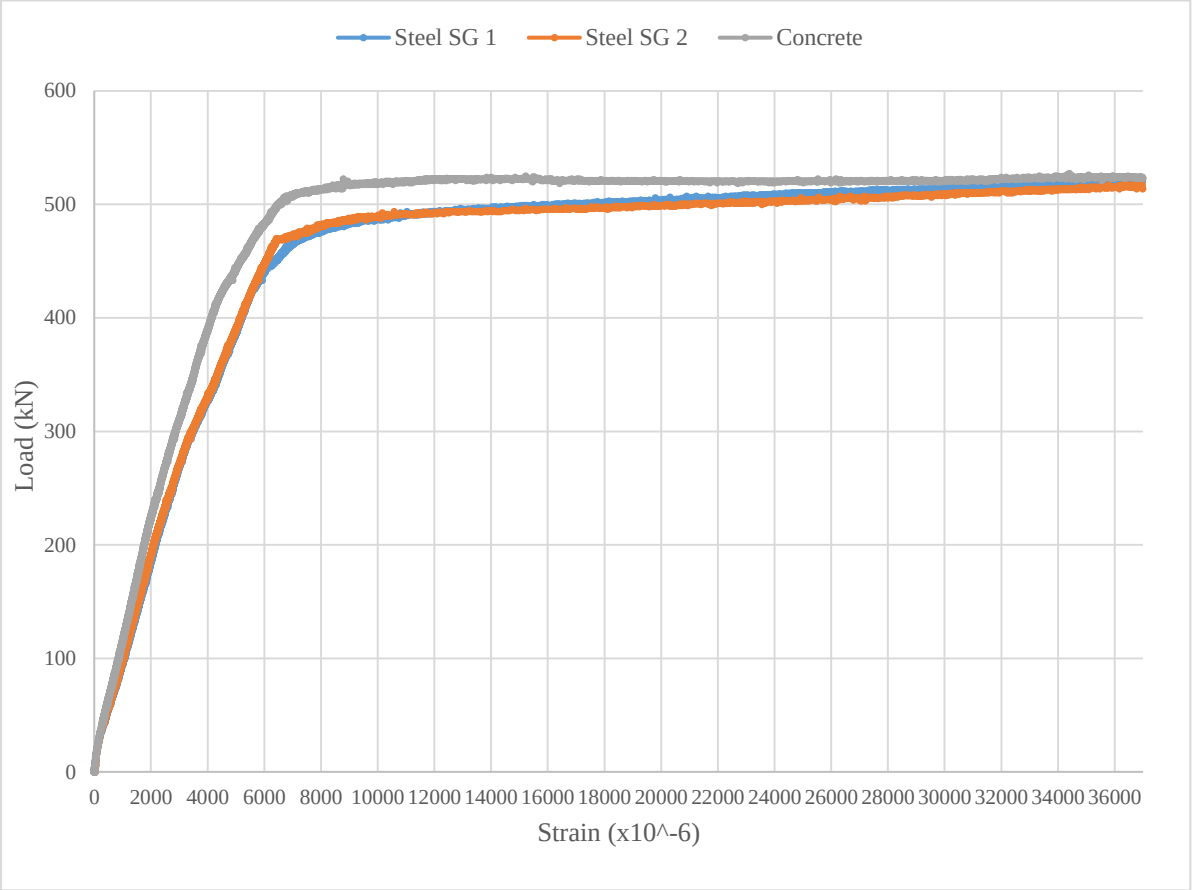

Figure 4.9 Column 1.5-C08-1 Load Strain Graph

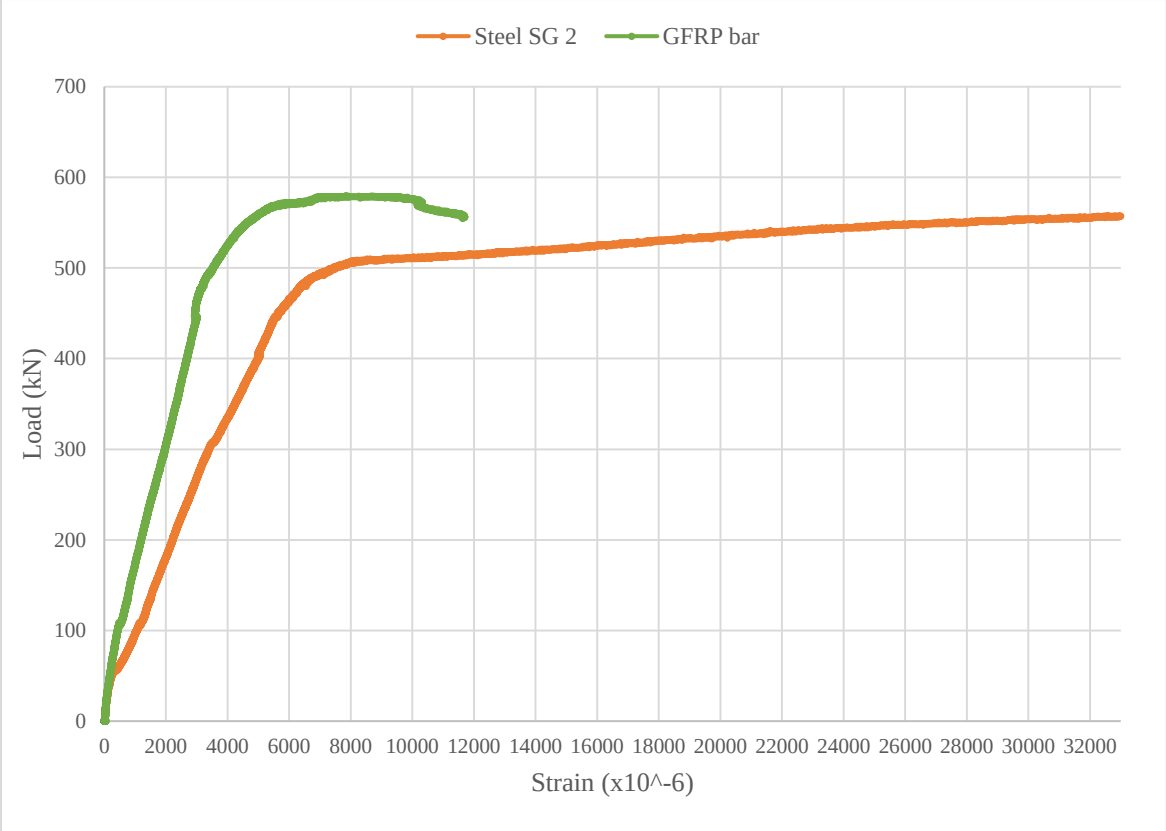

Figure 4.10 Column 1.5-C08-2 Load Strain Graph

4.2.3 Samples 1.5-C12

These two columns are strengthened with one NSM GFRP bar with a diameter of 12mm in the tension side of the column. They will be compared to the control samples to know the effects of GFRP bars, and the improvements obtained by strengthening. For the first column, cracks were formed in the middle of the column in the tension side at 580kN for the first column and 570kN for the second column as shown in Figure 4.11 and Figure 4.12 respectively. The cracks propagated into deeper cracks as the load increased, one crack widened and propagated until failure took place. The average failure load for the two columns is 575kN. A typical flexural failure was formed. For the first column, Figure 4.13, the LVDTs showed a maximum horizontal deflection of 19.3mm and maximum vertical deflection of 0.33mm in the column head and for the second column, Figure 4.14, LVDTs showed a maximum horizontal deflection of 17.4mm and maximum vertical deflection of 0.33mm in the column.

Figure 4.11 Cracks at the tension side of Column 1.5-C12-1

Figure 4.12 Cracks at the tension side of Column 1.5-C12-2

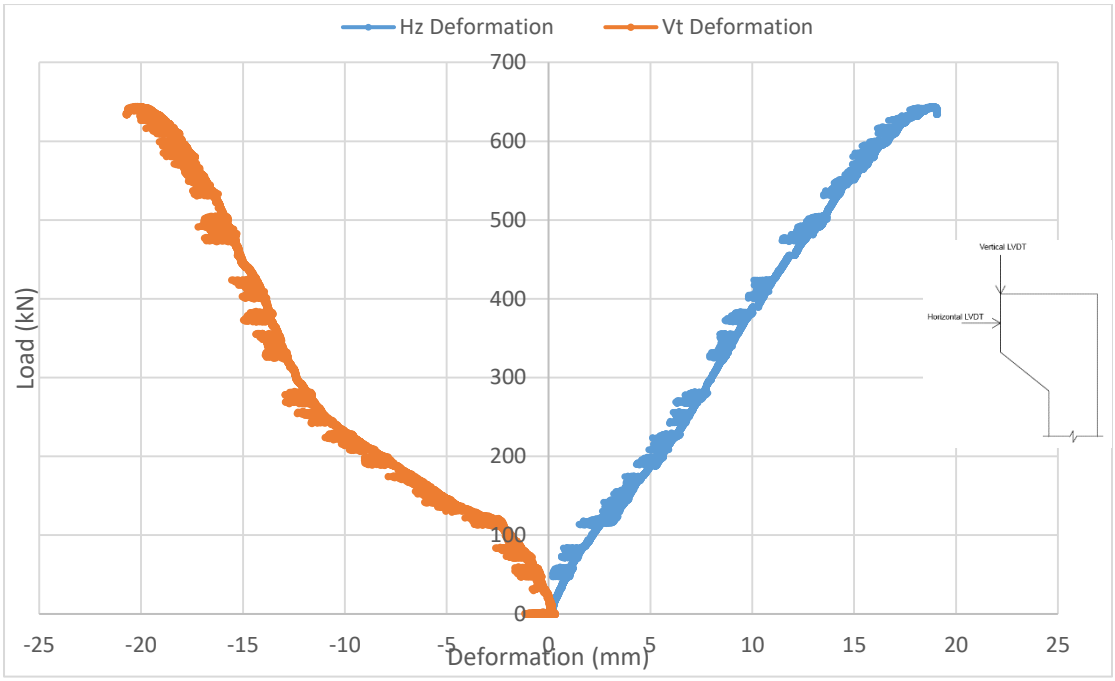

Figure 4.13 Sample 1.5-C12-1 Load-Deformation Graph

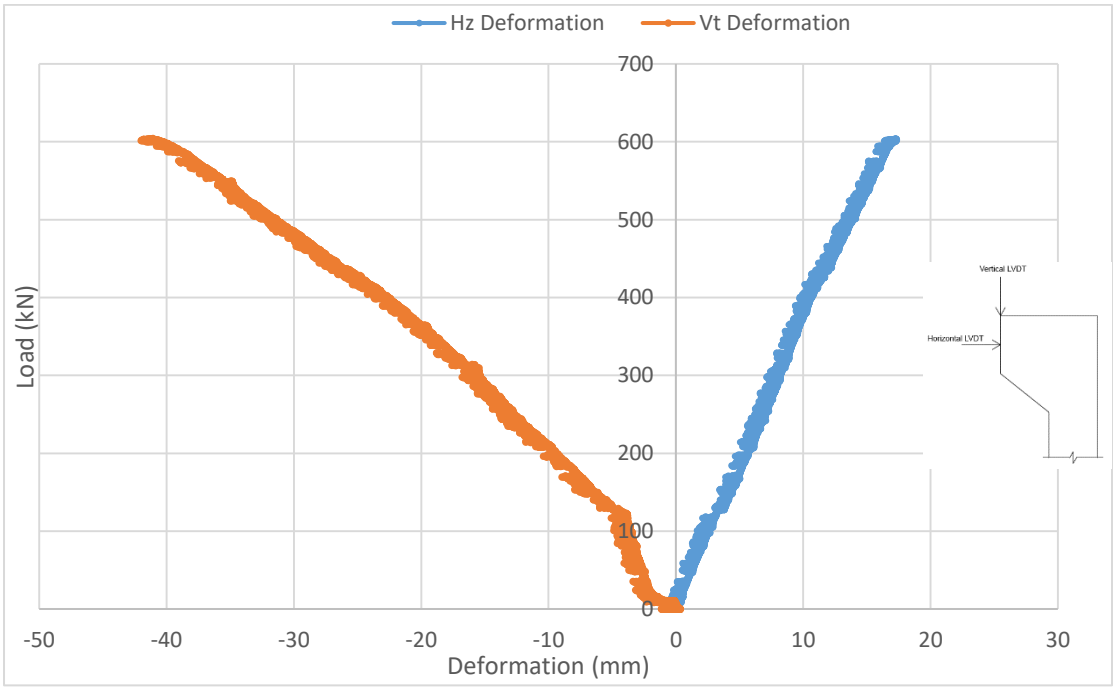

Figure 4.14 Sample 1.5-C12-2 Load-Deformation Graph

Figure 4.15 shows the load strain graph of the first column. It shows that the column cracking load is 120 kN, the failure load is 580 kN. With a steel yielding strain equal to 0.0018. The GFRP strain at failure load is 0.0095. Figure 4.16 shows the load

strain graph of the second column. It shows that the column cracking load is 180 kN, the failure load is 570 kN with a steel yielding strain equal to 0.0019. The GFRP strain at failure load is 0.0088. The load-strain graphs show that there was a jump in the strain at the failure load. This is because as the load increases the column deformation increases, hence increasing the eccentricity/second order effect on the columns. This causes the cracks to propagate and widen and therefore the stiffness of the column decreases. Thus, a jump in the strain is expected to occur.

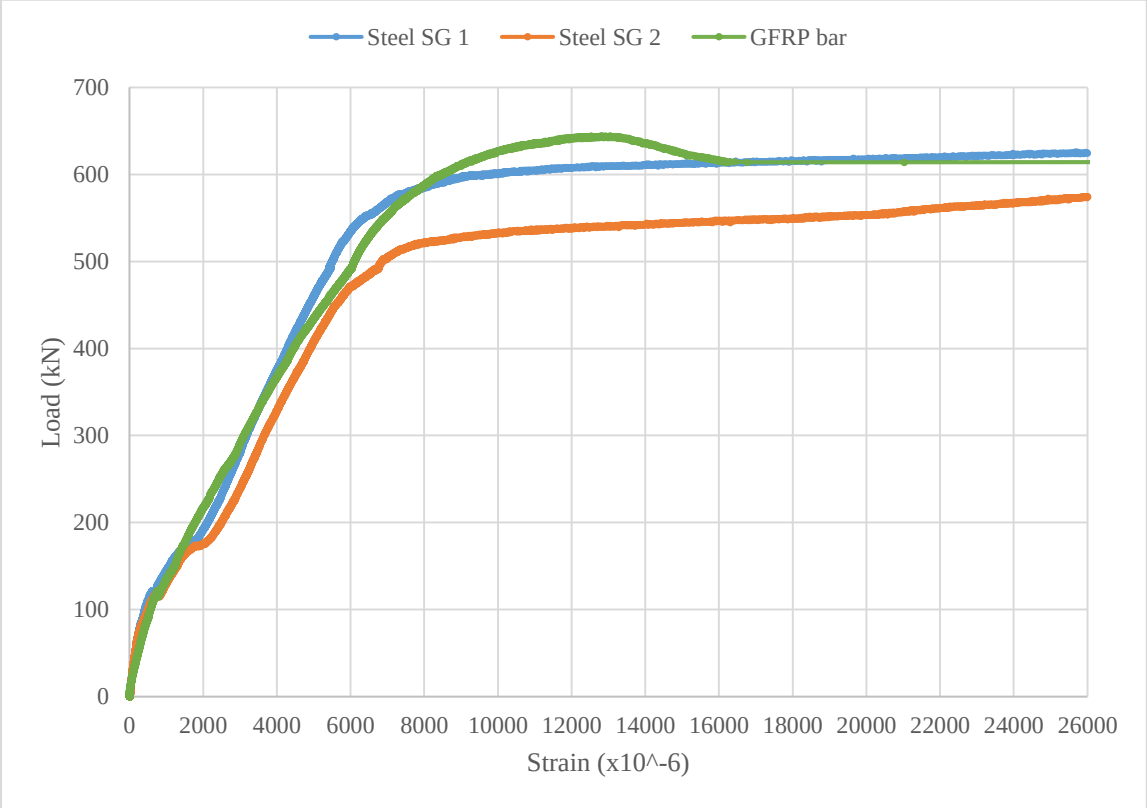

Figure 4.15 Column 1.5-C12-1 Load Strain Graph

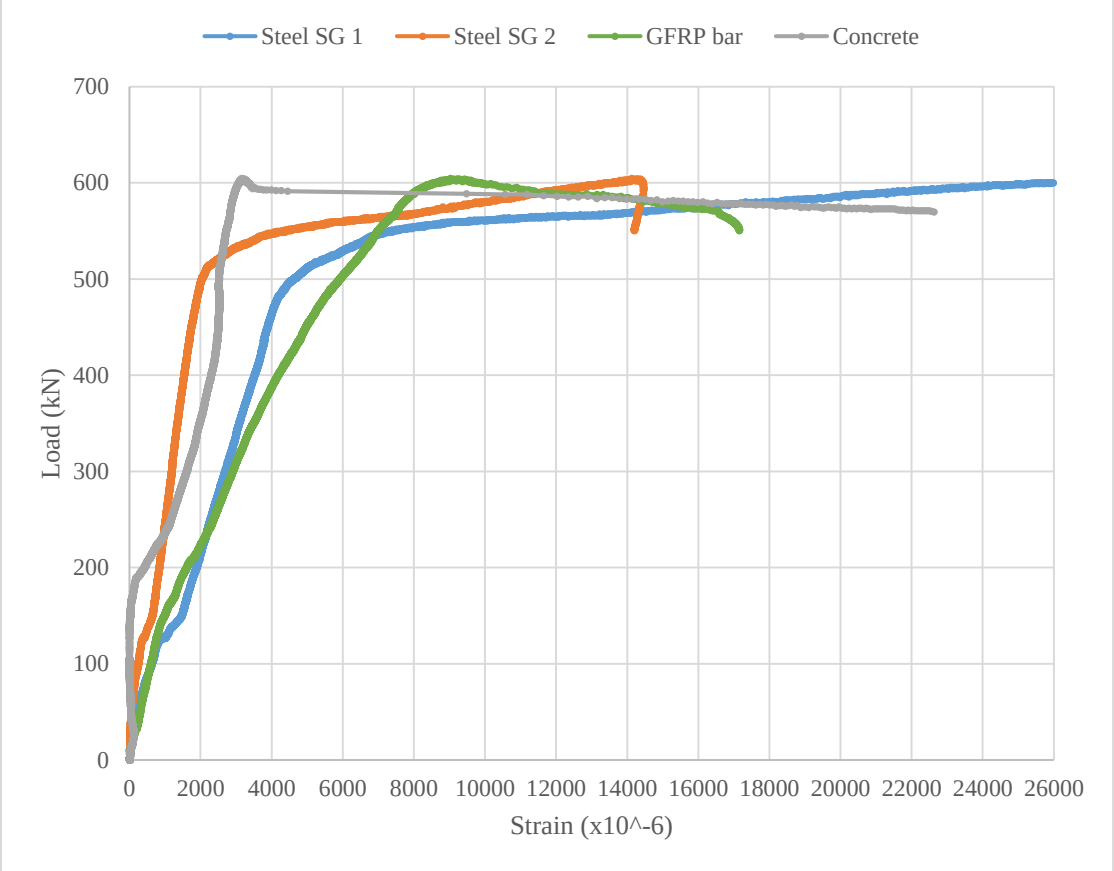

Figure 4.16 Column 1.5-C12-2 Load Strain Graph

4.2.4 Samples 2.0m C00

These two columns are strengthened with NSM GFRP bars. They act as control samples to be able to compare them to the other strengthened samples and know the effects of GFRP bars and the improvements obtained by strengthening. Cracks were formed in the middle of the column in the tension side at 410kN for the first column and 490kN for the second column as shown in Figure 4.17 and Figure 4.18 respectively. The cracks propagated into deeper cracks as the load increased, one crack widened and propagated until failure took place. The average failure load for the two columns is 450kN. A typical flexural failure was formed. For the first column, Figure 4.19, the LVDTs showed a maximum horizontal deflection of 20.2mm and maximum vertical deflection of 0.33mm in the column head and for the second column, Figure 4.20, LVDTs showed a maximum horizontal deflection of 15.3mm and maximum vertical deflection of 0.35mm in the column head.

Figure 4.17 Cracks at the tension side of Column 2-C00-1

Figure 4.18 Cracks at the tension side of Column 2-C00-2

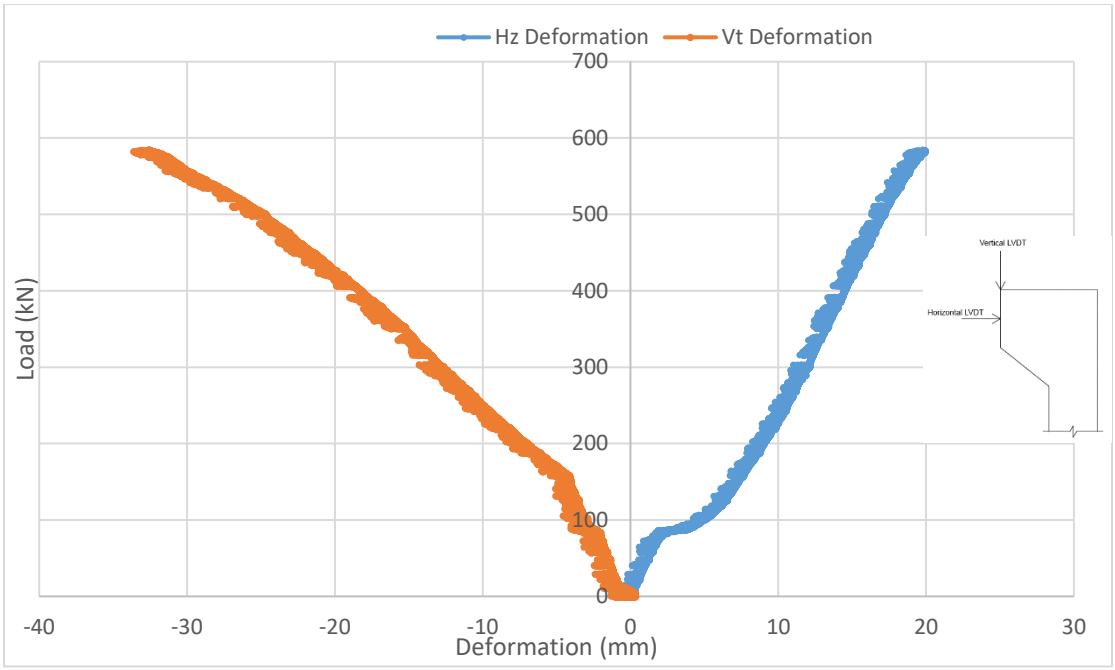

Figure 4.19 Sample 2.0-C00-1 Load-Deformation Graph

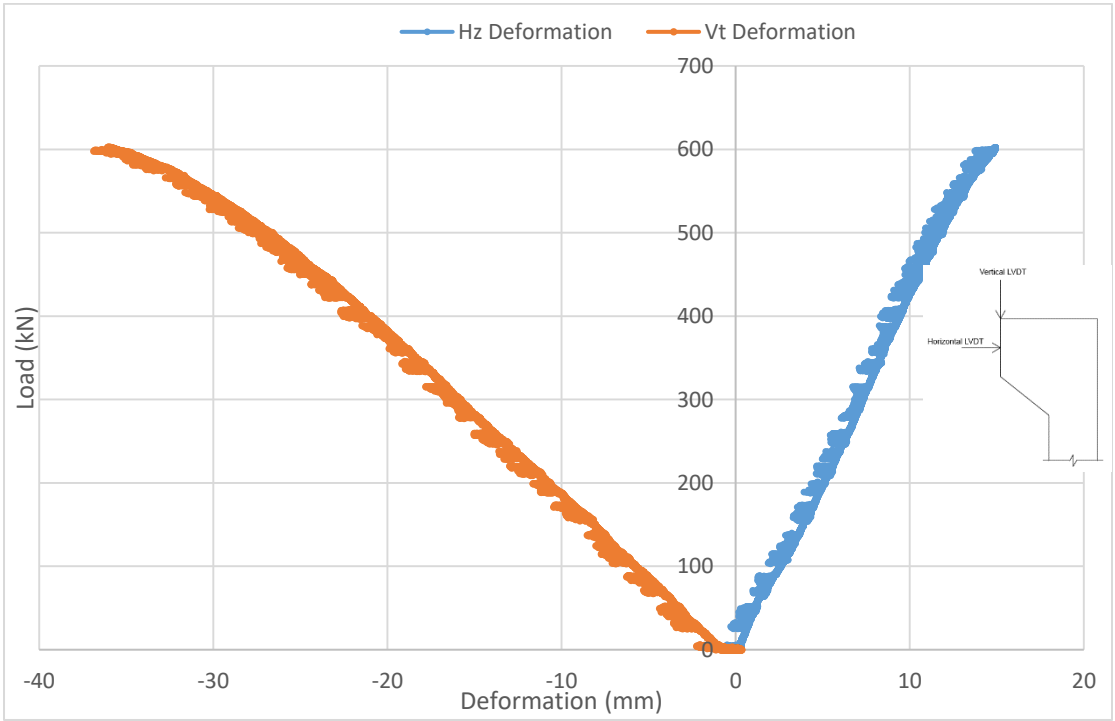

Figure 4.20 Sample 2.0-C00-2 Load-Deformation Graph

Figure 4.21 shows the load strain graph of the sample. It shows the load strain graph of the first column. It shows that the column cracking load is 100 kN, the failure

load is 410 kN, with a steel yielding strain equal to 0.0019. Figure 4.22 shows the load strain graph of the second column. It shows that the column cracking load is 100 kN, the failure load is 490 kN, with a steel yielding strain equal to 0.0018.

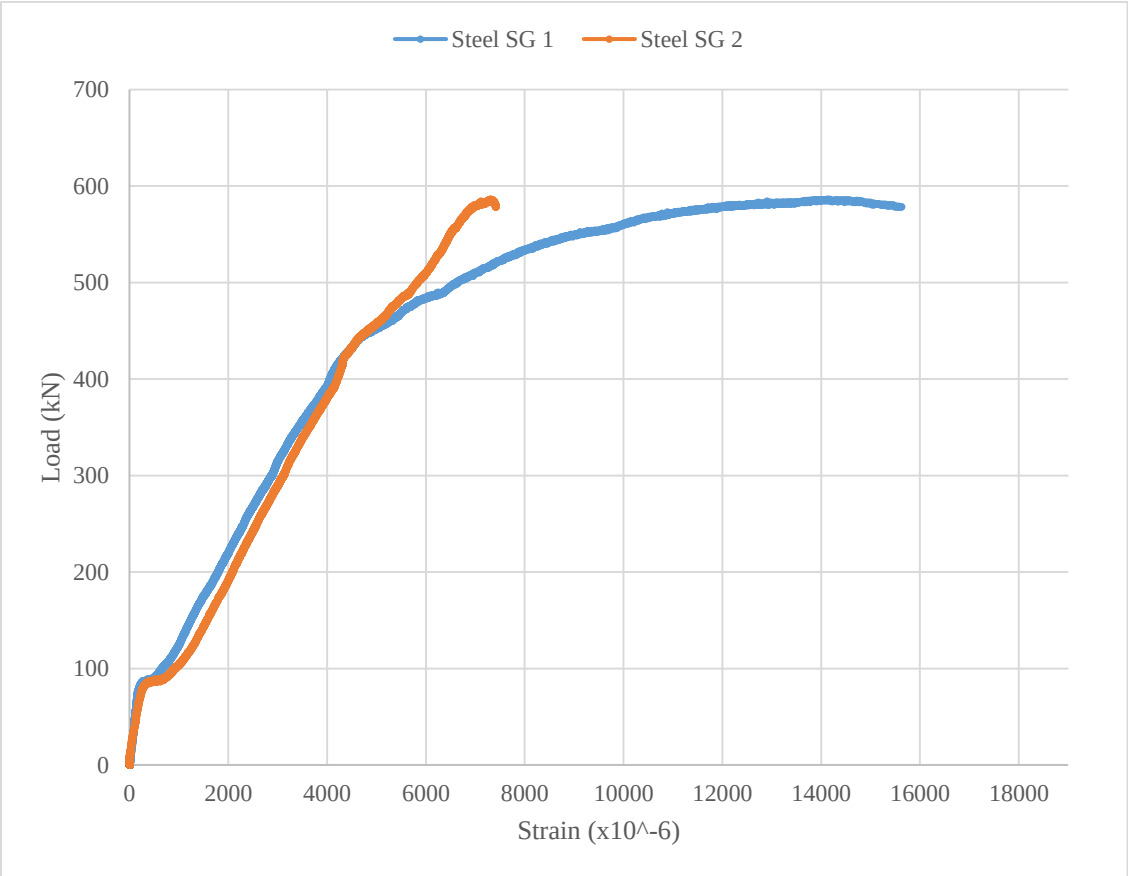

Figure 4.21 Column 2-C00-1 Load Strain Graph

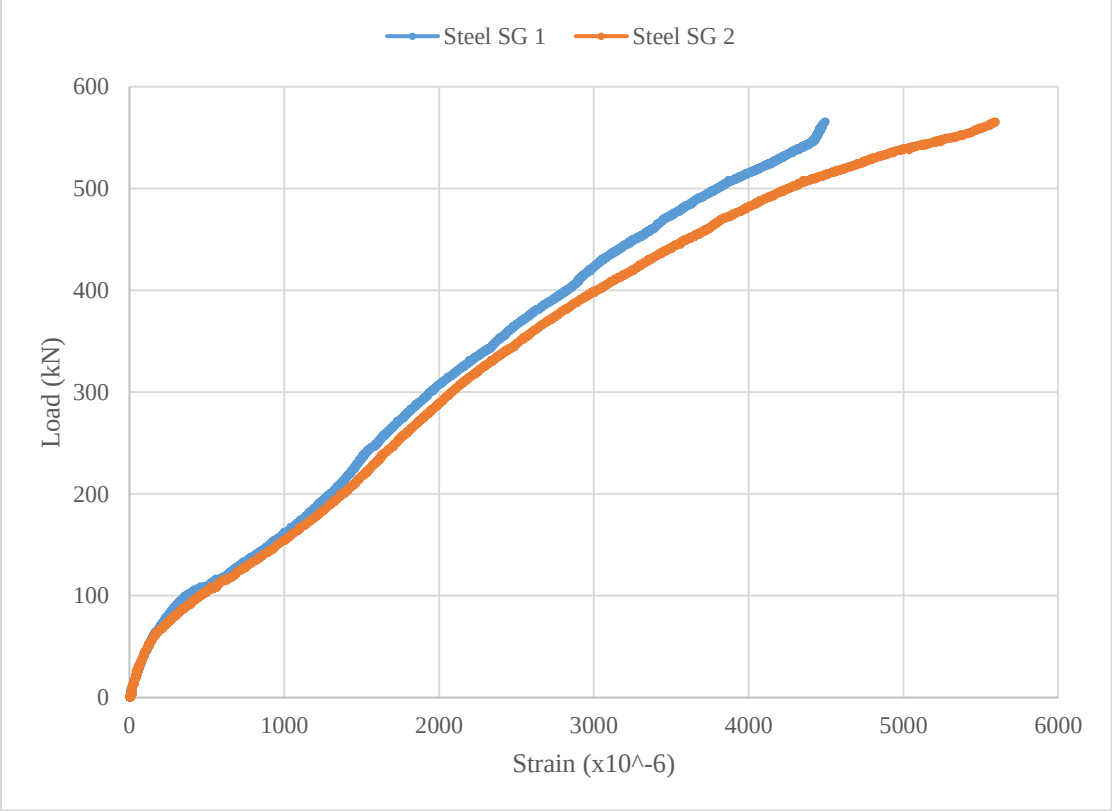

Figure 4.22 Column 2-C00-2 Load Strain Graph

4.2.5 Samples 2.0m C08

These two columns are strengthened with one NSM GFRP bar with a diameter of 8mm in the tension side of the column. They will be compared to the control samples to know the effects of GFRP bars, and the improvements obtained by strengthening. Cracks were formed in the middle of the column in the tension side at 640kN for the first column and 620kN for the second column as shown in Figure 4.23 and Figure 4.24 respectively. The cracks propagated into deeper cracks as the load increased, one crack widened and propagated until failure took place. The average failure load for the two columns is 630kN. A typical flexural failure was formed. For the first column, Figure 4.25, the LVDTs showed a maximum horizontal deflection of 15.6mm and maximum vertical deflection of 0.37mm in the column head and for the second column, Figure 4.28, the LVDTs showed a maximum horizontal deflection of 15.9mm and maximum vertical deflection of 0.33mm in the column head.

Figure 4.23 Cracks at the tension side of Column 2-C08-1

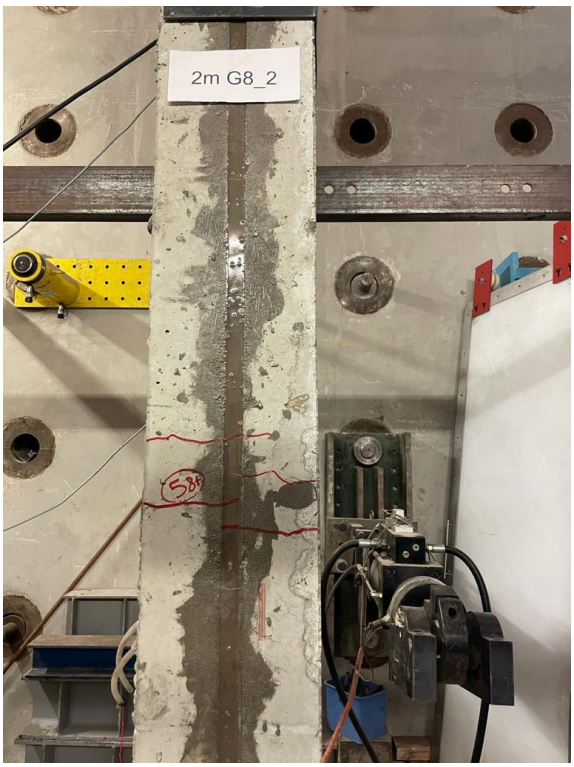

Figure 4.24 Cracks at the tension side of Column 2-C08-2

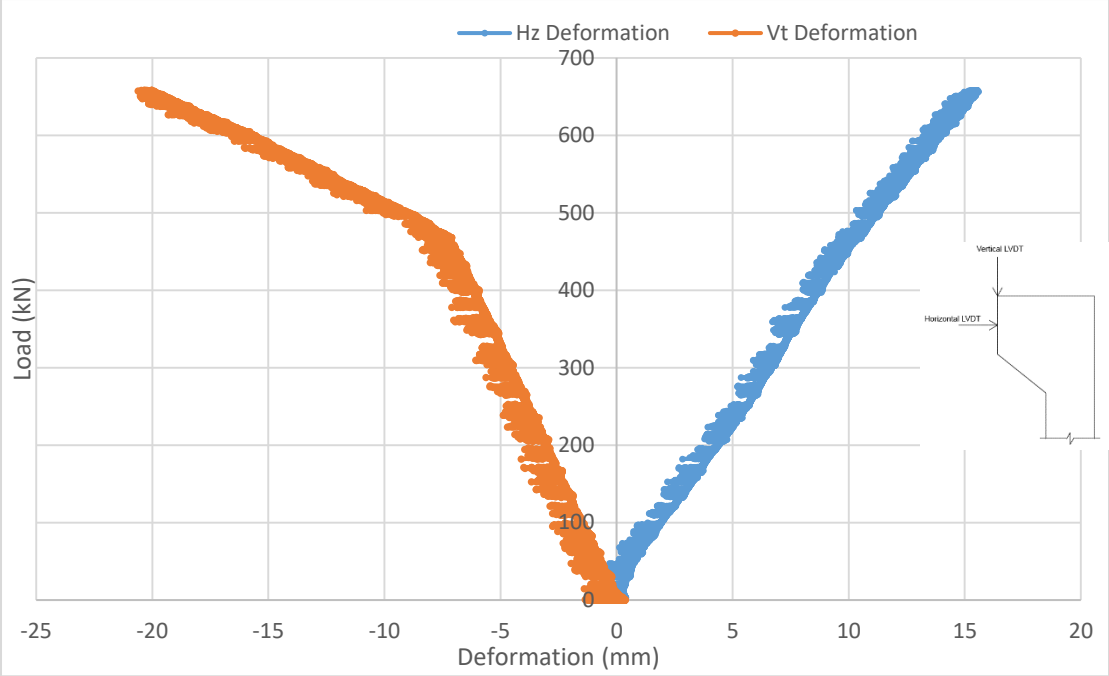

Figure 4.25 Sample 2.0-C08-1 Load-Deformation Graph

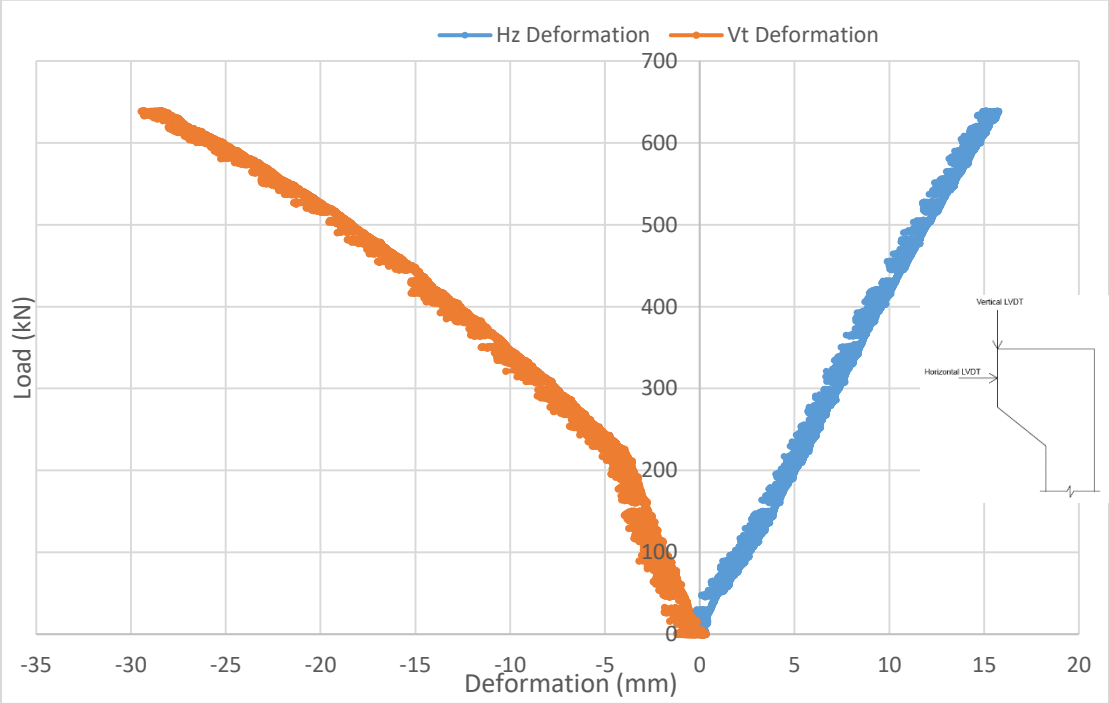

Figure 4.26 Sample 2.0-C08-2 Load-Deformation Graph

Figure 4.27 shows the load strain graph of the first column. It shows that the column cracking load is 120 kN, the failure load is 640 kN, with a steel yielding strain

equal to 0.002. The GFRP strain at failure load is 0.01. Figure 4.28 shows the load strain graph of the second column. It shows that the column cracking load is 80 kN, the failure load is 620 kN, with a steel yielding strain equal to 0.0022. The GFRP strain at failure load is 0.01. The load-strain graphs show that there was a jump in the strain at the failure load. This is because as the load increases the column deformation increases, hence increasing the eccentricity/second order effect on the columns. This causes the cracks to propagate and widen and therefore the stiffness of the column decreases. Thus, a jump in the strain is expected to occur.

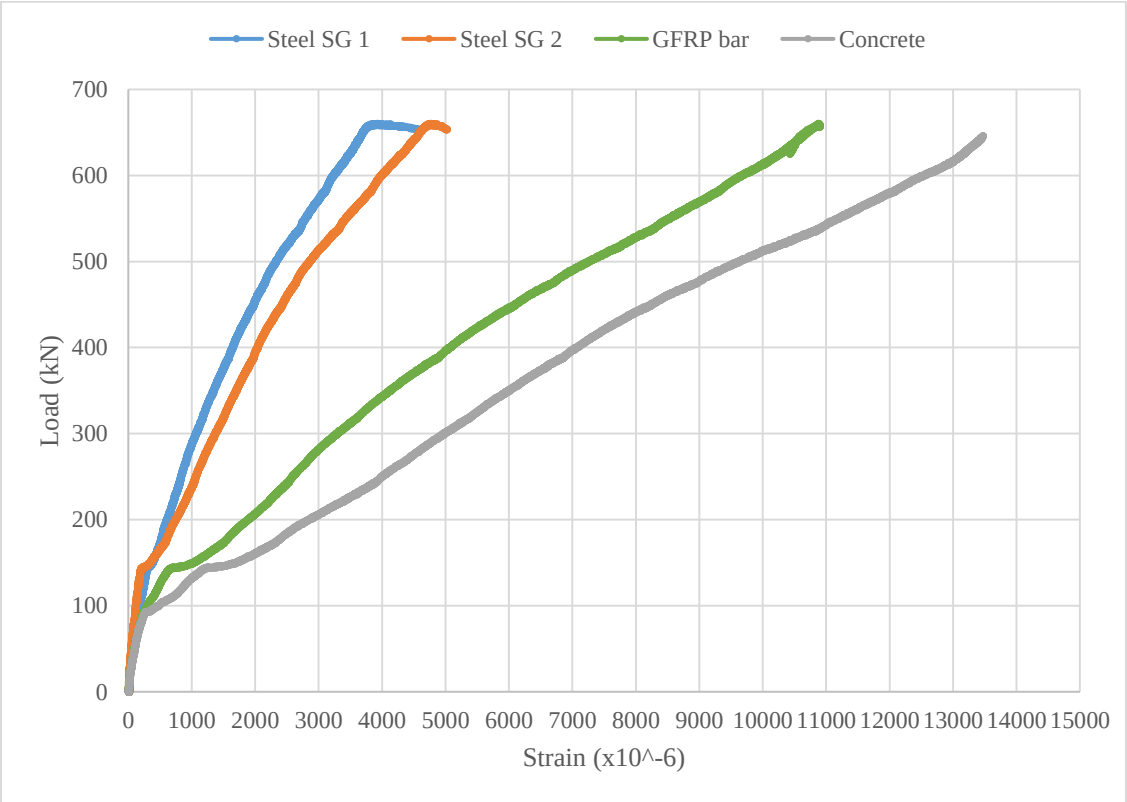

Figure 4.27 Column 2.-C08-1 Load Strain Graph

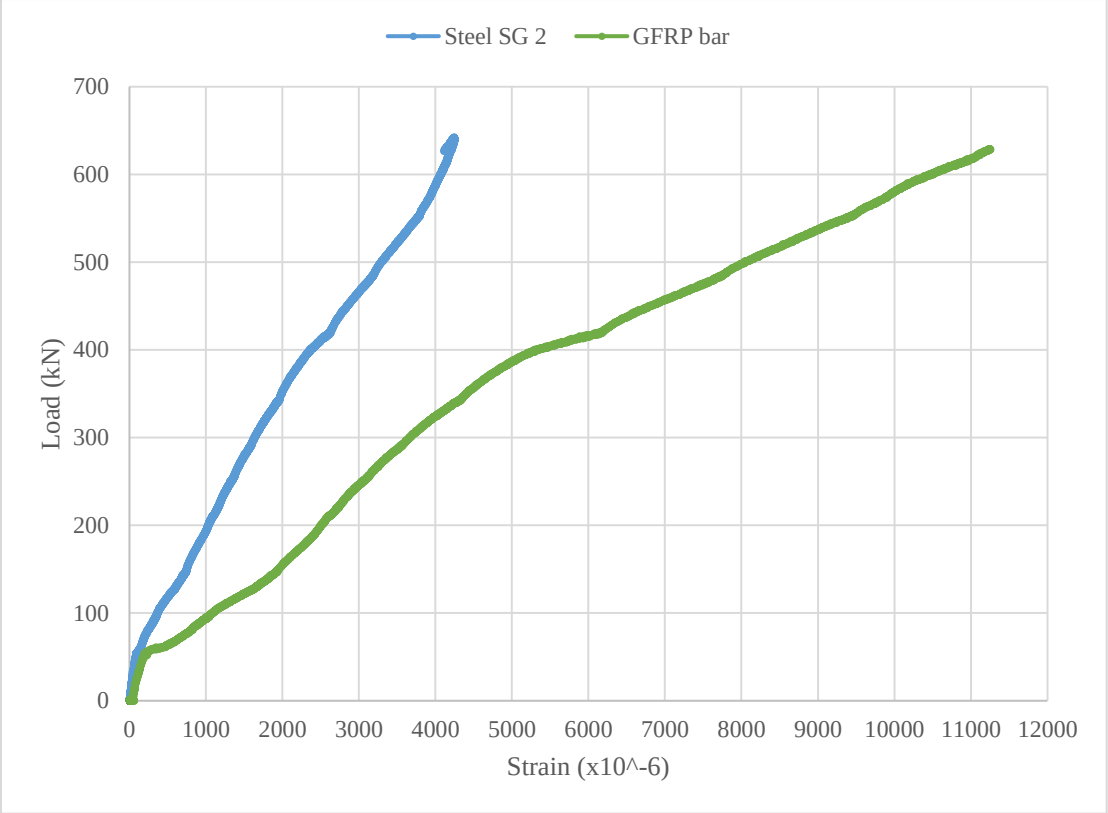

Figure 4.28 Column 2-C08-2 Load Strain Graph

4.2.6 Samples 2.0m C12

These two samples are strengthened with one NSM GFRP bar with a diameter of 12mm in the tension side of the column. They will be compared to the control samples to know the effects of GFRP bars, and the improvements obtained by strengthening. Cracks were formed in the middle of the column in the tension side at 600kN for the first column and 600kN for the second column as shown in Figure 4.29 and Figure 4.30 respectively. The cracks propagated into deeper cracks as the load increased, one crack widened and propagated until failure took place. The average failure load for the two columns is 600kN. A typical flexural failure was formed. For the first column, Figure 4.33, the LVDTs showed a maximum horizontal deflection of 15mm and maximum vertical deflection of 0.35mm in the column head and for the second column, Figure 4.32, LVDTs showed a maximum horizontal deflection of 15.3mm and maximum vertical deflection of 0.27mm in the column head.

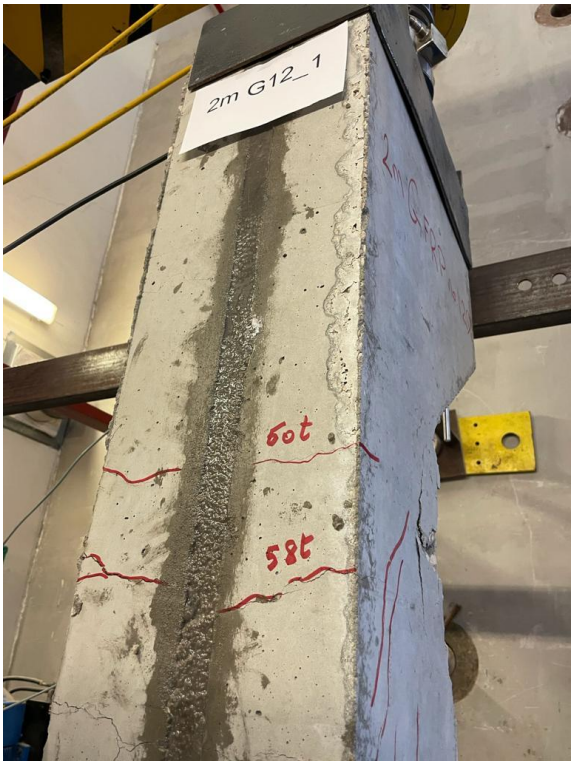

Figure 4.29 Cracks at the tension side of Column 2-C12-1

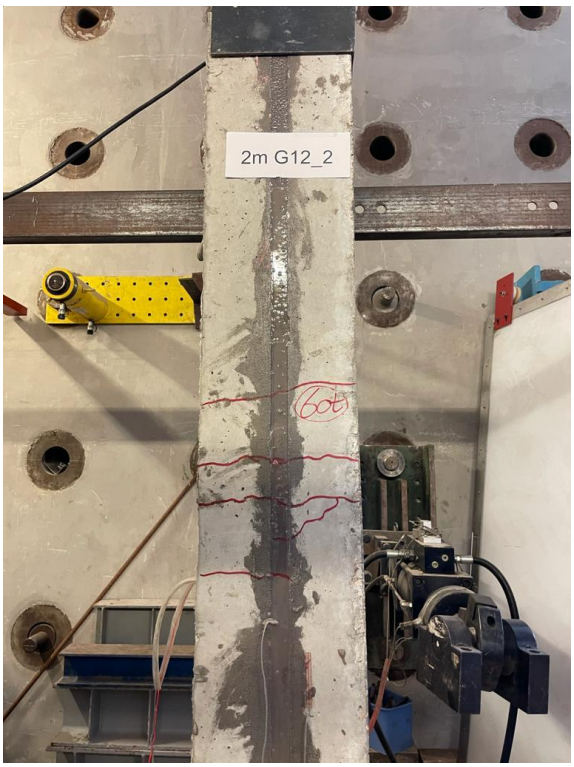

Figure 4.30 Cracks at the tension side of Column 2-C12-2

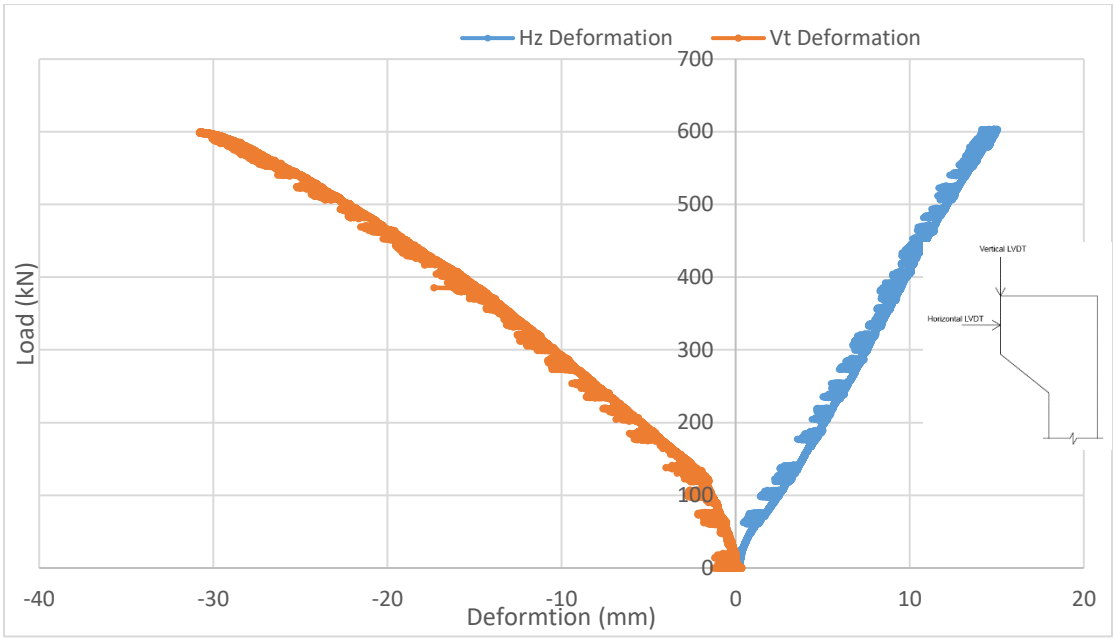

Figure 4.31 Sample 2.0-C12-1 Load-Deformation Graph

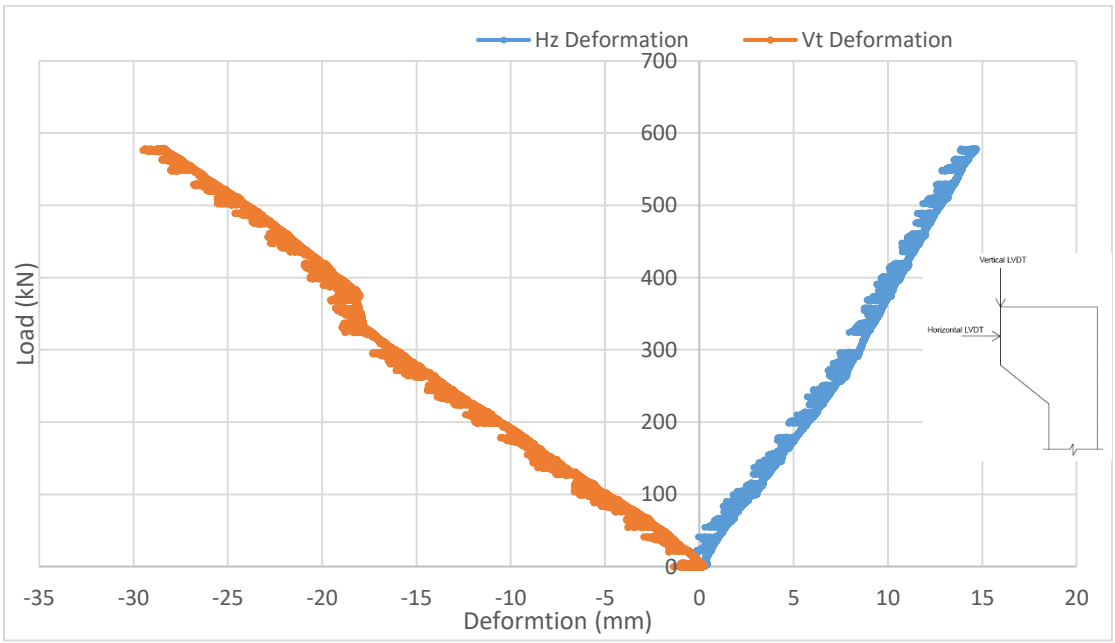

Figure 4.32 Sample 2.0-C12-2 Load-Deformation Graph

Figure 4.33 shows the load strain graph of the first column. It shows that the column cracking load is 80 kN, the failure load is 600 kN, with steel yielding strain equal to 0.002. The GFRP strain at failure load is 0.0087. Figure 4.34 shows the load strain graph of the second column. It shows that the column cracking load is 100 kN,

the failure load is 600 kN, with a steel yielding strain equal to 0.00175. The GFRP strain at failure load is 0.01. The load-strain graphs show that there was a jump in the strain at the failure load. This is because as the load increases the column deformation increases, hence increasing the eccentricity/second order effect on the columns. This causes the cracks to propagate and widen and therefore the stiffness of the column decreases. Thus, a jump in the strain is expected to occur.

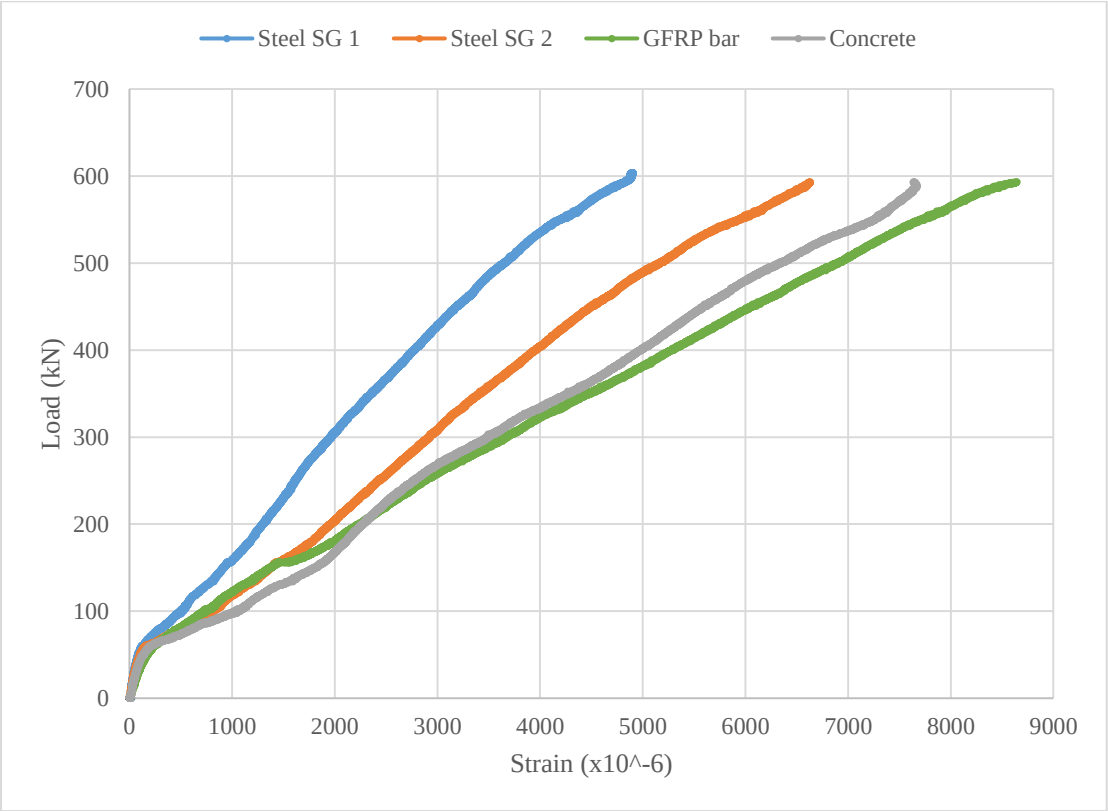

Figure 4.33 Column 2-C12-1 Load Strain Graph

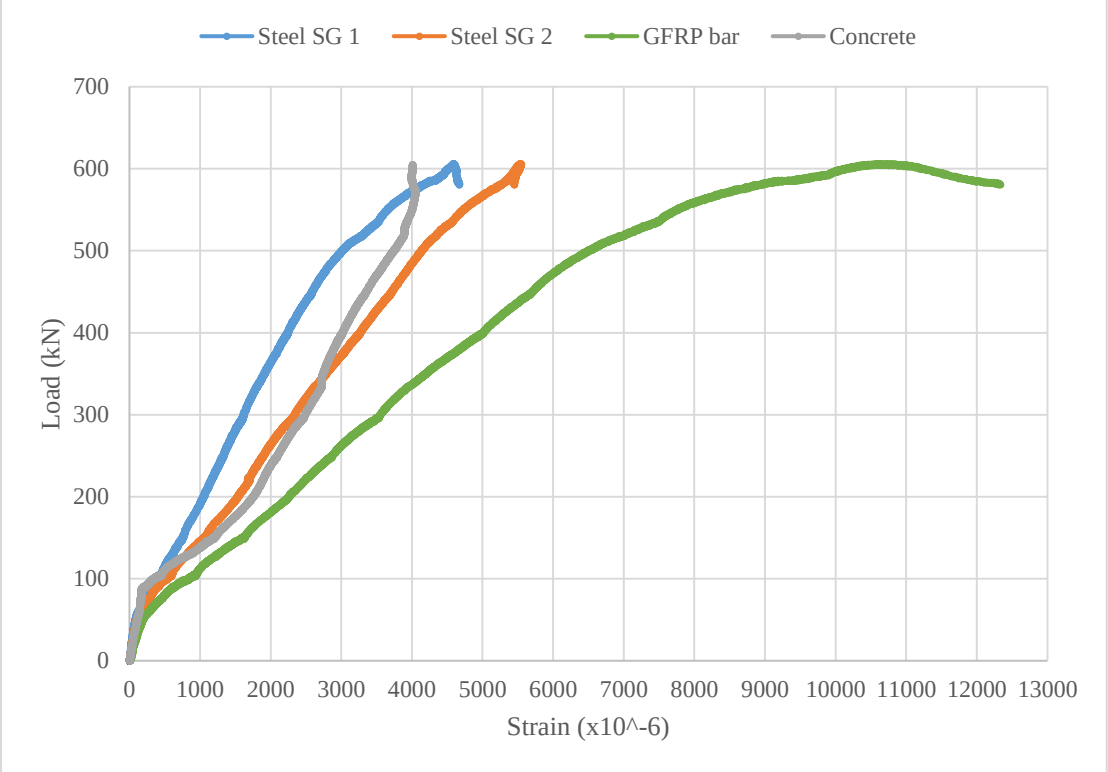

Figure 4.34 Column 2-C12-2 Load Strain Graph

4.2.7 Samples 2.5m C00

These two samples strengthened with NSM GFRP bars. They act as control samples to be compared to the other strengthened samples and know the effects of adding NSM GFRP bars and the improvements obtained by strengthening. Cracks were formed in the middle of the column in the tension side at 440kN for the first column and 440kN for the second column as shown in Figure 4.35 and Figure 4.36 respectively. The cracks propagated into deeper cracks as the load increased, one crack widened and propagated until failure took place. The average failure load for the two columns is 440kN. A typical flexural failure was formed. For the first column, Figure 4.37, the LVDTs showed a maximum horizontal deflection of 17.5mm and maximum vertical deflection of 0.35mm in the column head and for the second column, Figure 4.38, LVDTs showed a maximum horizontal deflection of 12.5mm and maximum vertical deflection of 0.35mm in the column head.

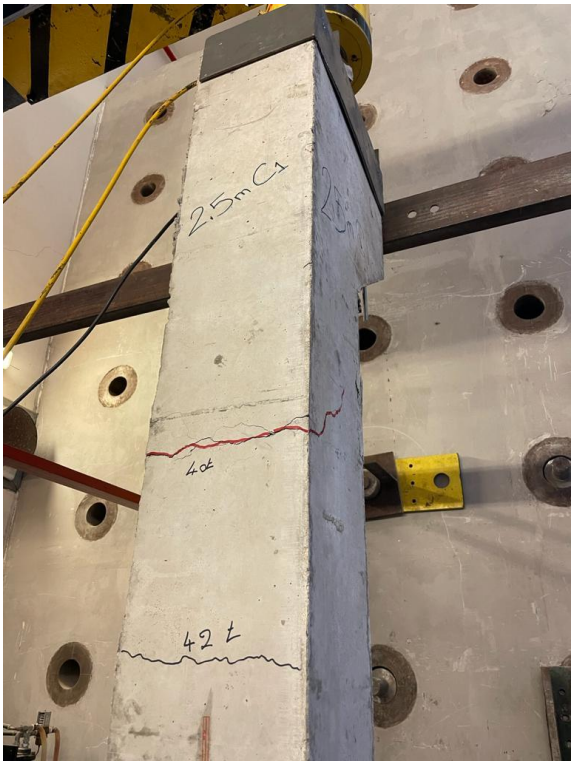

Figure 4.35 Cracks at the tension side of Column 2.5-C00-1

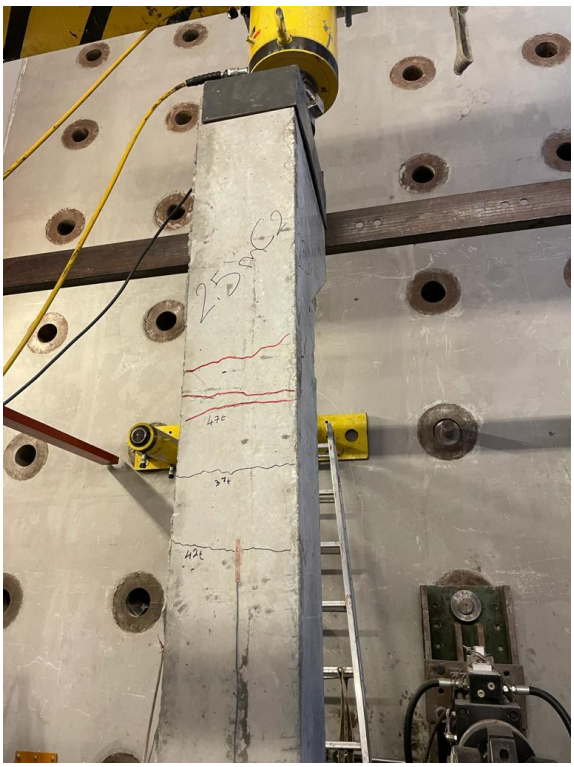

Figure 4.36 Cracks at the tension side of Column 2.5-C00-2

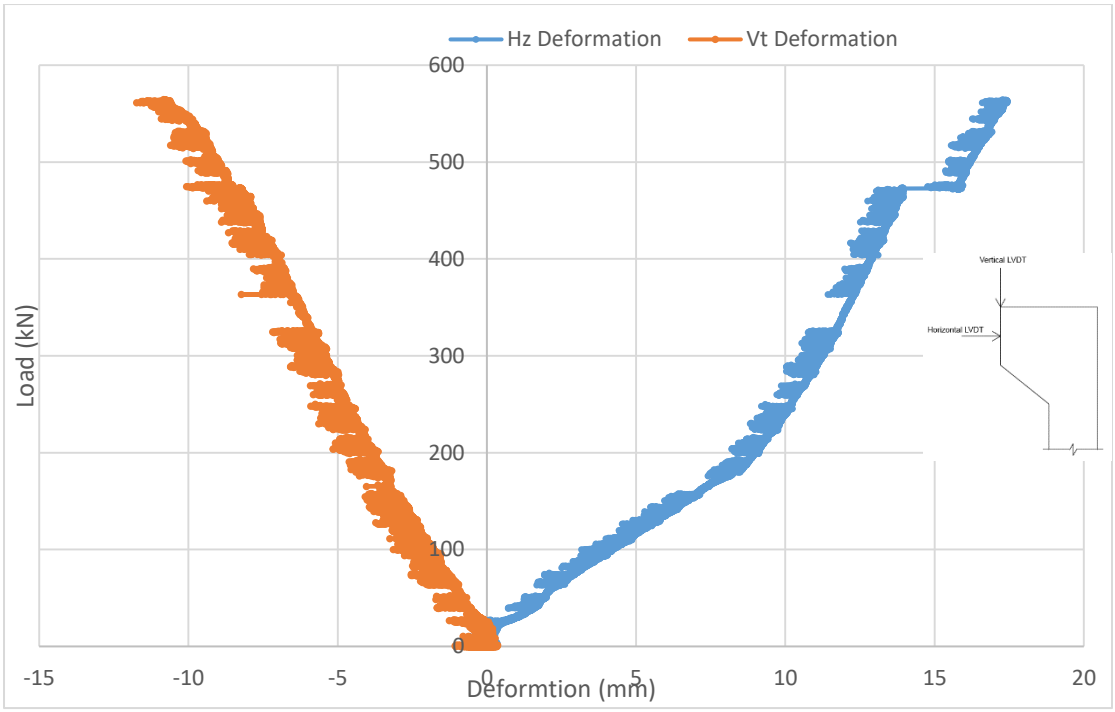

Figure 4.37 Sample 2.5-C00-1 Load-Deformation Graph

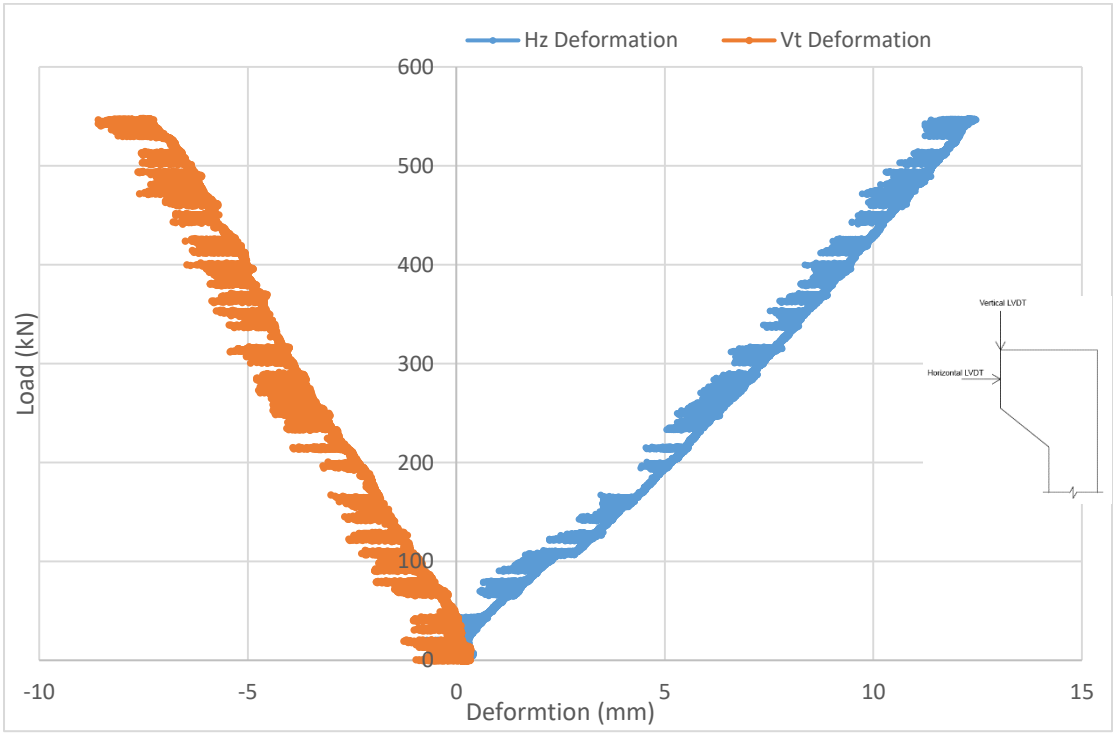

Figure 4.38 Sample 2.5-C00-2 Load-Deformation Graph

Figure 4.39 shows the load strain graph of the first column. It shows that the column cracking load is 100 kN, the failure load is 440 kN, with a steel yielding strain equal to 0.0024. Figure 4.40 shows the load strain graph of the second column. It shows that the column cracking load is 100 kN, the failure load is 440 kN with a steel yielding strain equal to 0.0019.

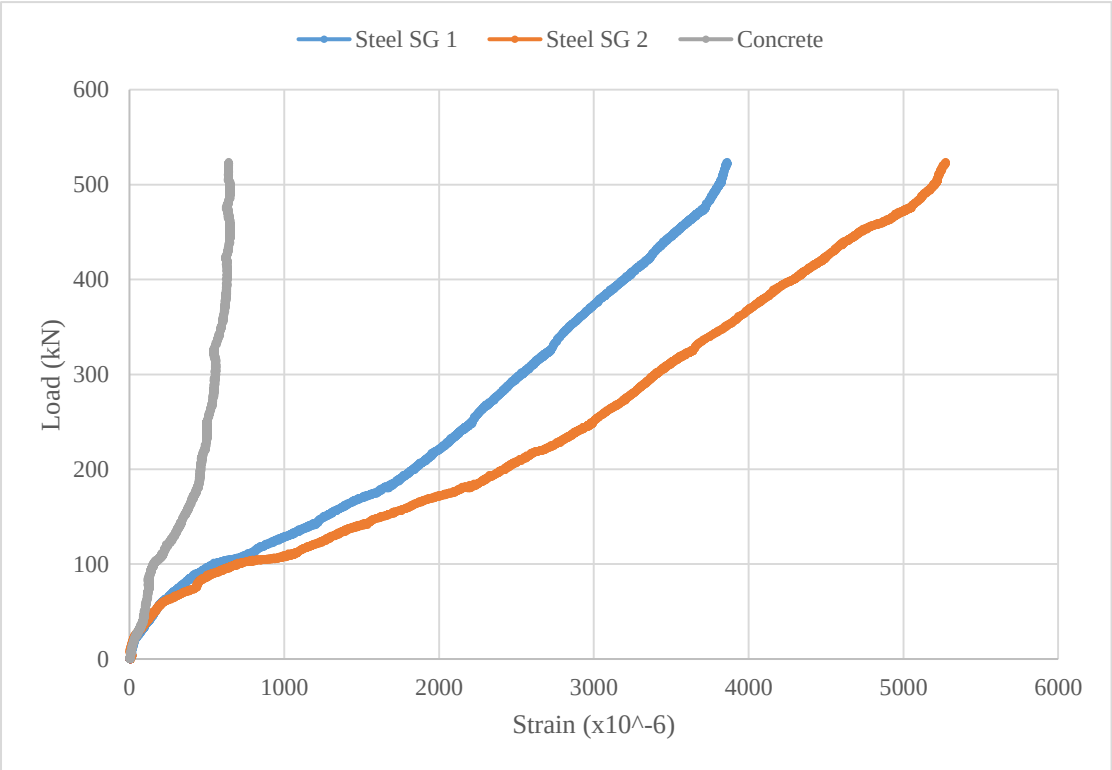

Figure 4.39 Column 2.5-C00-1 Load Strain Graph

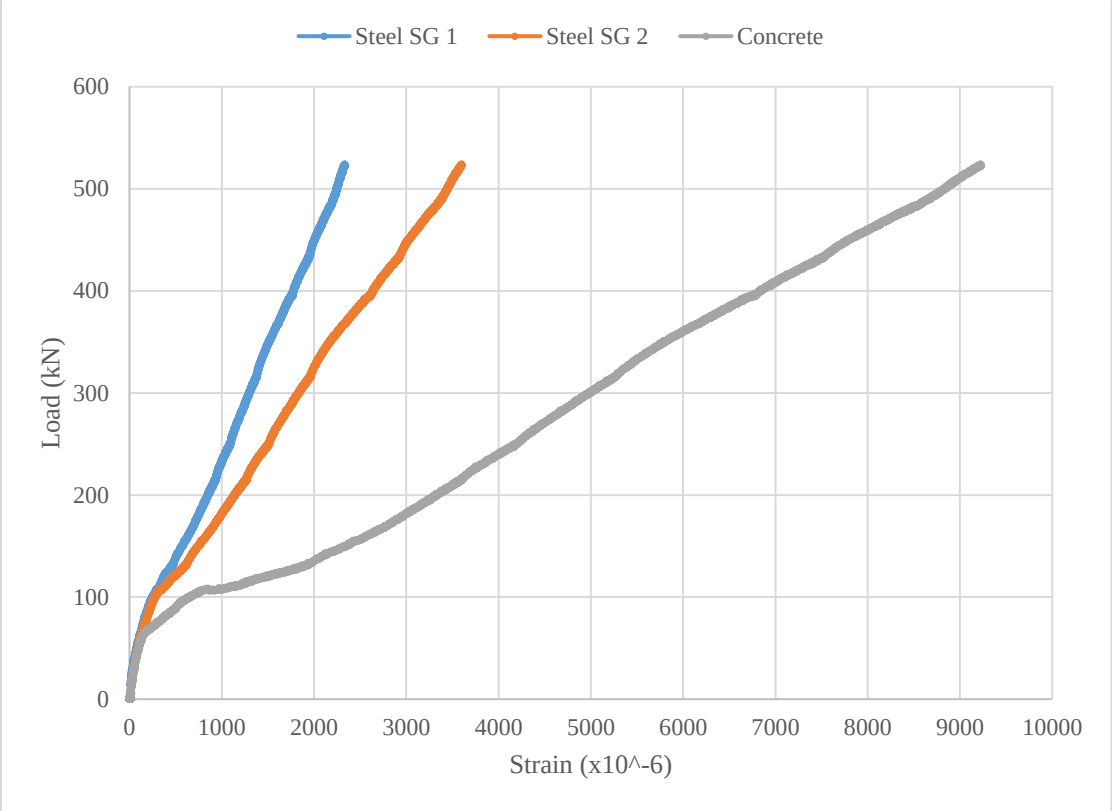

Figure 4.40 Column 2.5-C00-2 Load Strain Graph

4.2.8 Samples 2.5m C08

These two samples are strengthened with one NSM GFRP bar with a diameter of 8mm in the tension side of the column. They are compared to the control samples to know the effects of NSM GFRP bars, and the improvements obtained by strengthening. Cracks were formed in the middle of the column in the tension side at 490kN for the first column and 510kN for the second column as shown in Figure 4.41 and Figure 4.42 respectively. The cracks propagated into deeper cracks as the load increased, one crack widened and propagated until failure took place. The two columns had an average failure load of 500kN. A typical flexural failure was formed. For the first column, Figure 4.45, the LVDTs showed a maximum horizontal deflection of 12.5mm and maximum vertical deflection of 0.35mm in the column head and for the second column, Figure 4.46, LVDTs showed a maximum horizontal deflection of 11.8mm and maximum vertical deflection of 0.88mm in the column head.

Figure 4.41 Cracks at the tension side of Column 2.5-C08-1

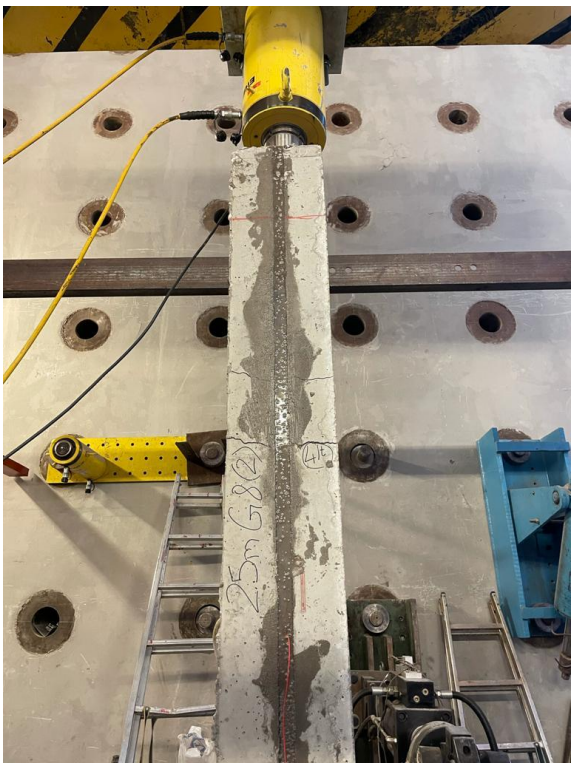

Figure 4.42 Cracks at the tension side of Column 2.5-C08-2

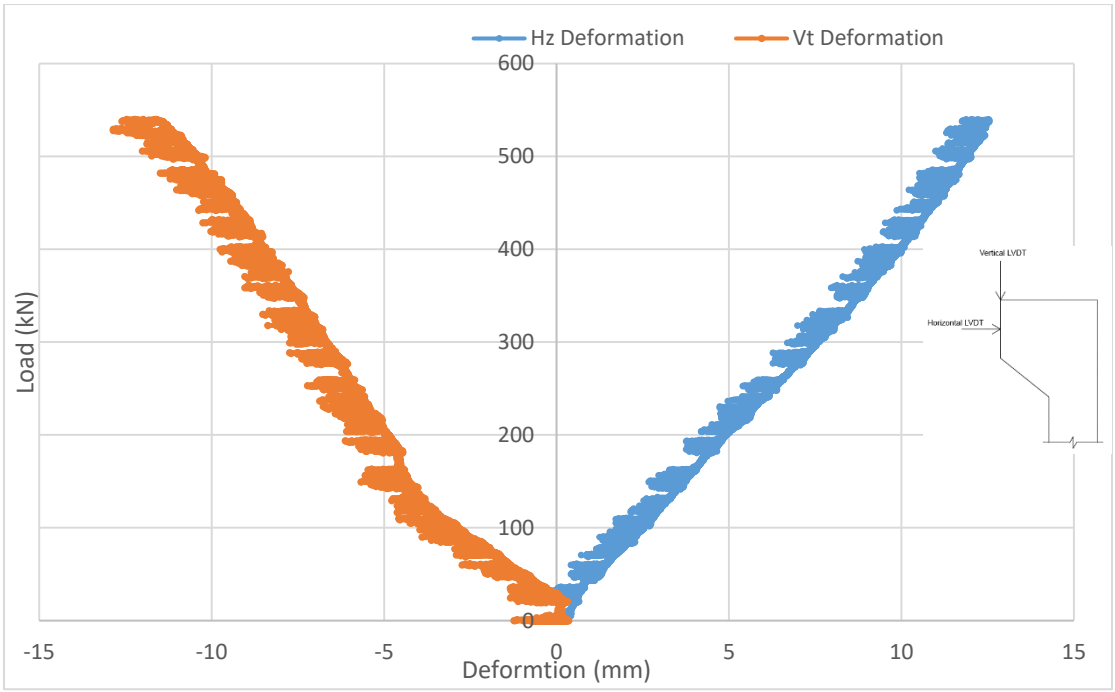

Figure 4.43 Sample 2.5-C08-1 Load-Deformation Graph

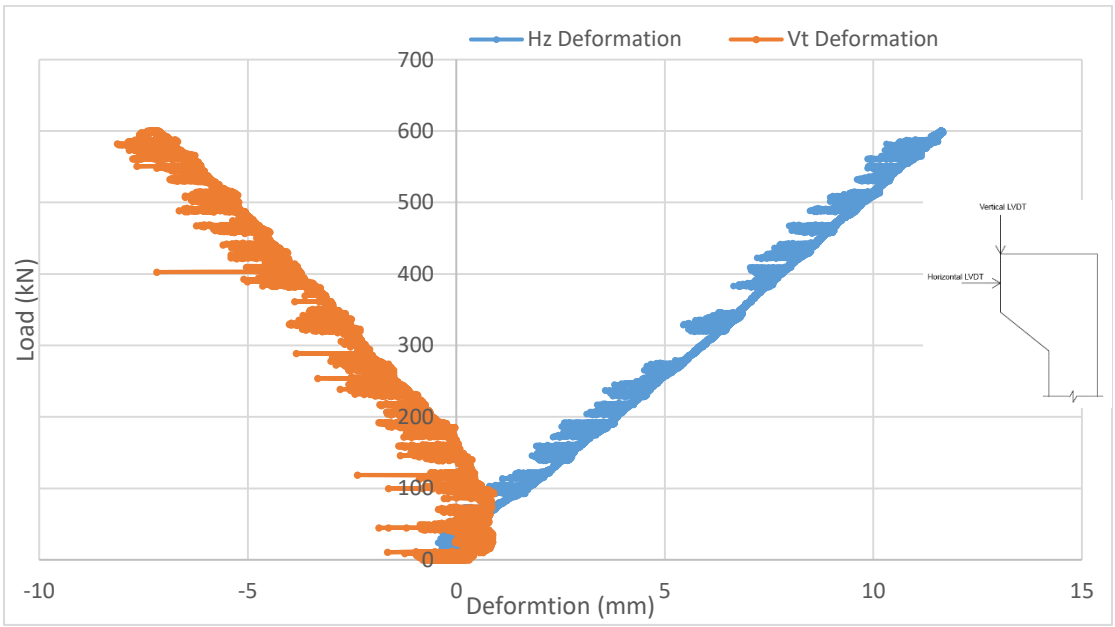

Figure 4.44 Sample 2.5-C08-2 Load-Deformation Graph

Figure 4.45 shows the load strain graph of the first column. It shows that the column cracking load is 100 kN, the failure load is 490 kN, with a steel yielding strain equal to 0.002. The GFRP strain at failure load is 0.003. Figure 4.46 shows the load

strain graph of the second column. It shows that the column cracking load is 100 kN, the failure load is 510 kN, with a steel yielding strain equal to 0.0019. The GFRP strain at failure load is 0.0007. The load-strain graphs show that there was a jump in the strain at the failure load. This is because as the load increases the column deformation increases, hence increasing the eccentricity/second order effect on the columns. This causes the cracks to propagate and widen and therefore the stiffness of the column decreases. Thus, a jump in the strain is expected to occur.

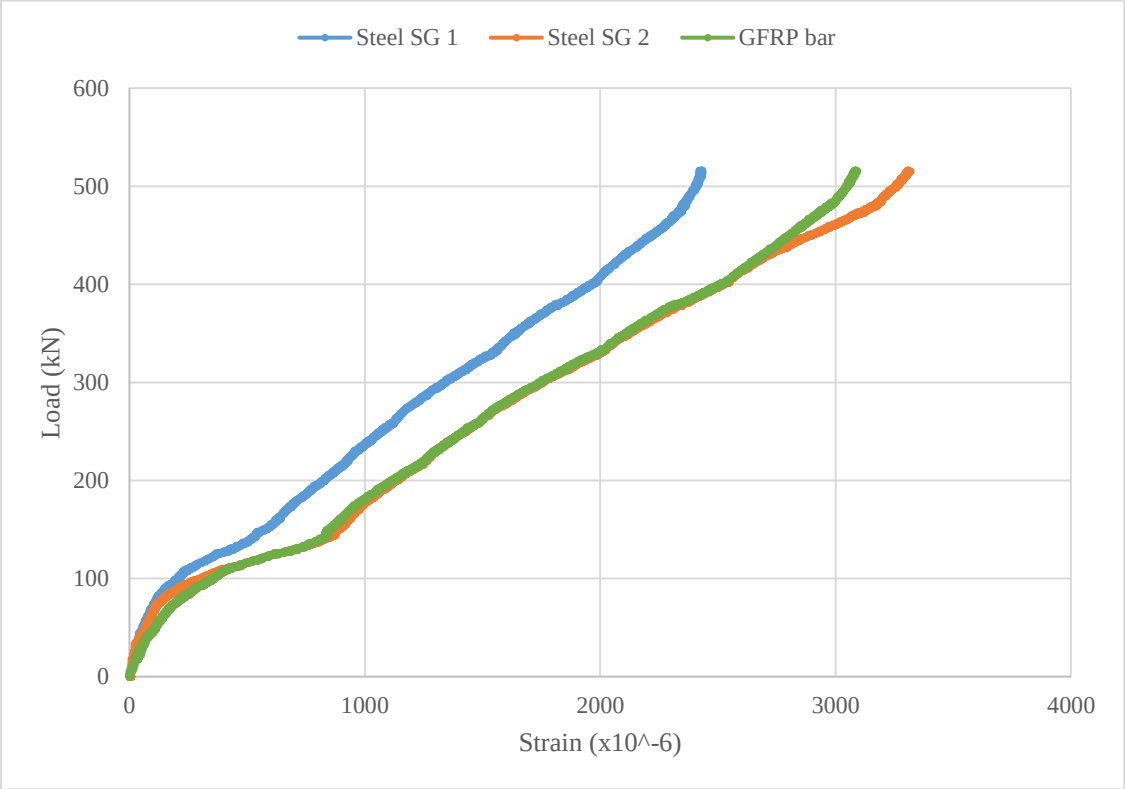

Figure 4.45 Column 2.5-C08-1 Load Strain Graph

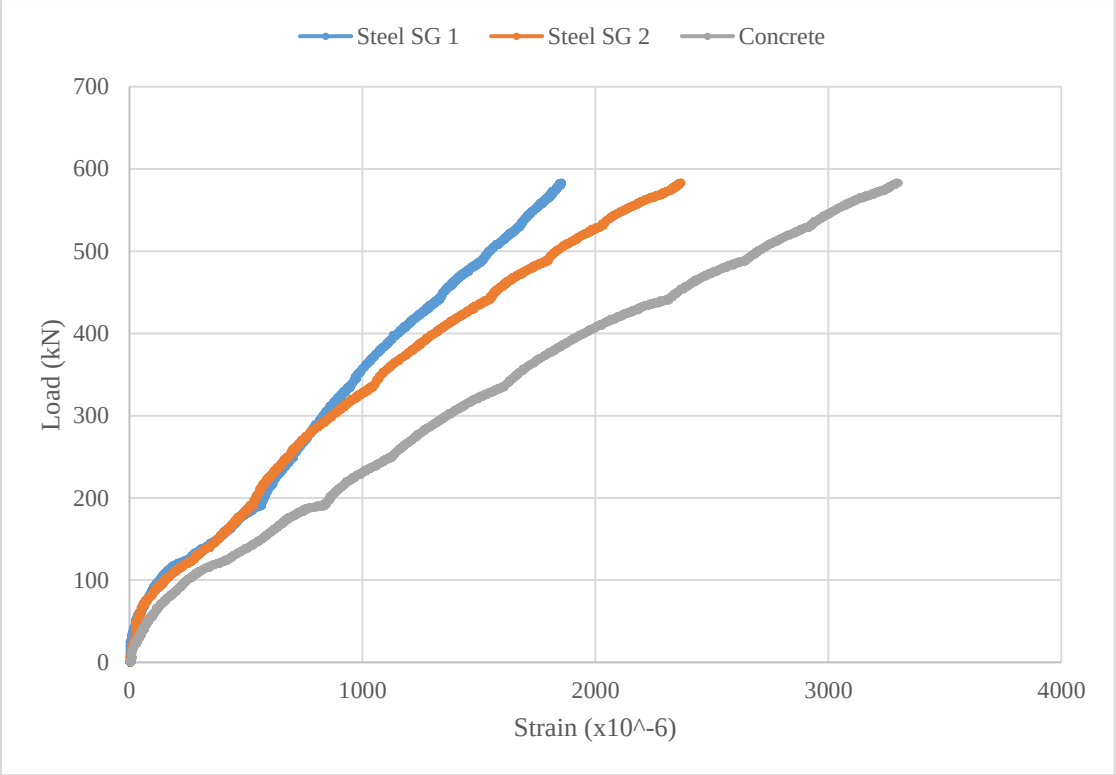

Figure 4.46 Column 2.5-C08-2 Load Strain Graph

4.2.9 Sample 2.5m C12

This column is reinforced with main and transverse reinforcement and is strengthened with one GFRP bar with a diameter of 12mm in the tension side of the column. It will be compared to the control samples to know the effects of GFRP bars, and the improvements obtained by strengthening. Cracks were formed in the middle of the column in the tension side at as shown in Figure 4.47. The cracks propagated into deeper cracks as the load increased, one crack widened and propagated until failure took place at a load of 580 kN. A typical flexural failure was formed. The LVDTs showed a maximum horizontal deflection of 0.35mm and maximum vertical deflection of 0.41mm in the column head.

Figure 4.47 Cracks at the tension side of Column 2.5-C12

Figure 4.48 shows the load strain graph of the column. It shows that the column cracking load is 110 kN, the failure load is 590 kN, with a steel yielding strain equal to 0.0021. The GFRP strain at failure load is 0.01. The load-strain graphs show that there was a jump in the strain at the failure load. This is because as the load increases the column deformation increases, hence increasing the eccentricity/second order effect on the columns. This causes the cracks to propagate and widen and therefore the stiffness of the column decreases. Thus, a jump in the strain is expected to occur.

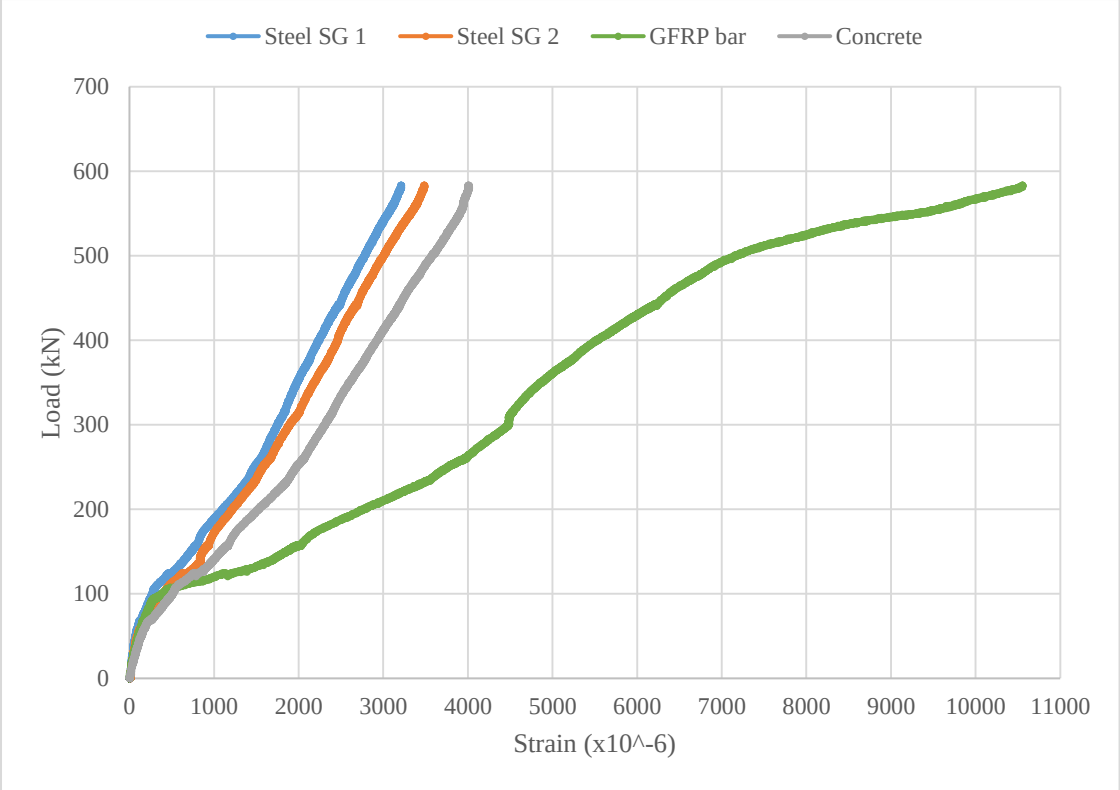

Figure 4.48 Column 2.5-C12 Load Strain Graph

4.3 Discussion

Table 4.1shows the slenderness of each column, the GFRP reinforcement ratio (µ-GFRP) and the results of all samples in terms of the failure loads, the maximum horizontal and vertical deflections, and the steel yield strain. The table reveals that for the same slenderness, the failure load increases as the µ-GFRP increases. It also shows that the deflection decreases as the slenderness increases.

Table 4.1 Summary of Sample Results

Sample ID	$\lambda = \frac{kl}{r}$	µ-GFRP	Failure Load (kN)	Max vl deflection (mm)	Max hz deflection (mm)	Steel Yield Strain
1.5-C00-1	12	0	430	19	16	0.0022
1.5-C00-2	12	0	-	30	19	-
1.5-C08-1	12	0.0008	520	33	15	0.0021
1.5-C08-2	12	0.0008	530	13	17.6	0.0019
1.5-C12-1	12	0.0018	580	20	19	0.0018

Sample ID	$\lambda = \frac{kl}{r}$	μ-GFRP	Failure Load (kN)	Max vl deflection (mm)	Max hz deflection (mm)	Steel Yield Strain
1.5-C12-2	12	0.0018	570	40	16	0.0019
2.0-C00-1	16	0	410	33	20	0.0019
2.0-C00-2	16	0	490	35	15	0.0018
2.0-C08-1	16	0.0008	620	21	16	0.0020
2.0-C08-2	16	0.0008	630	28	16	0.0022
2.0-C12-1	16	0.0018	600	31	15	0.0020
2.0-C12-2	16	0.0018	600	27	15.3	0.0018
2.5-C00-1	20	0	440	13	15	0.0024
2.5-C00-2	20	0	440	8	12.5	0.0019
2.5-C08-1	20	0.0008	490	13	12.5	0.0020
2.5-C08-2	20	0.0008	510	8	11.8	0.0019
2.5-C12-1	20	0.0018	580	-	-	0.0021

4.3.1 General Enhancement of Column Strength

4.3.1.1 1.5m Column Comparison (effect of GFRP ratio)

Figure 4.49 shows that for the same column height (slenderness) the failure load of the 1.5m column increased from 430 kN for the control sample to an average of 525 kN for the no.8 GFRP strengthened column. This is an increase of 22%. The no. 12 GFRP strengthened column failed at an average load of 575 kN. This is an increase of 34% compared to the control column and 10% compared to the no.8 GFRP strengthened column. Therefore, as seen in Figure 4.50, as the μ-GFRP increases, the percentage of strength enhancement increases.

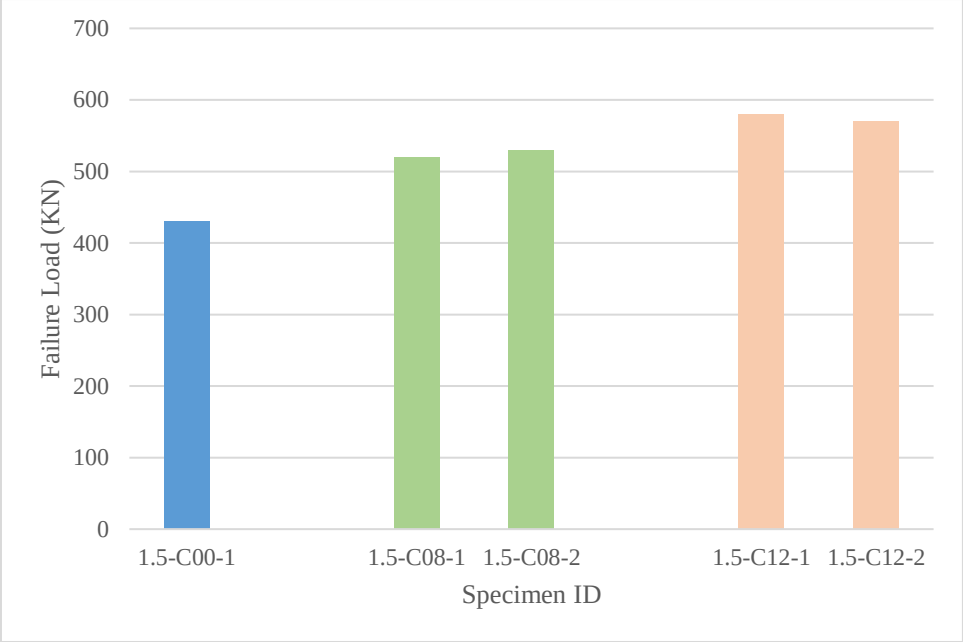

Figure 4.49 (1.5m) Column Failure Load Comparison

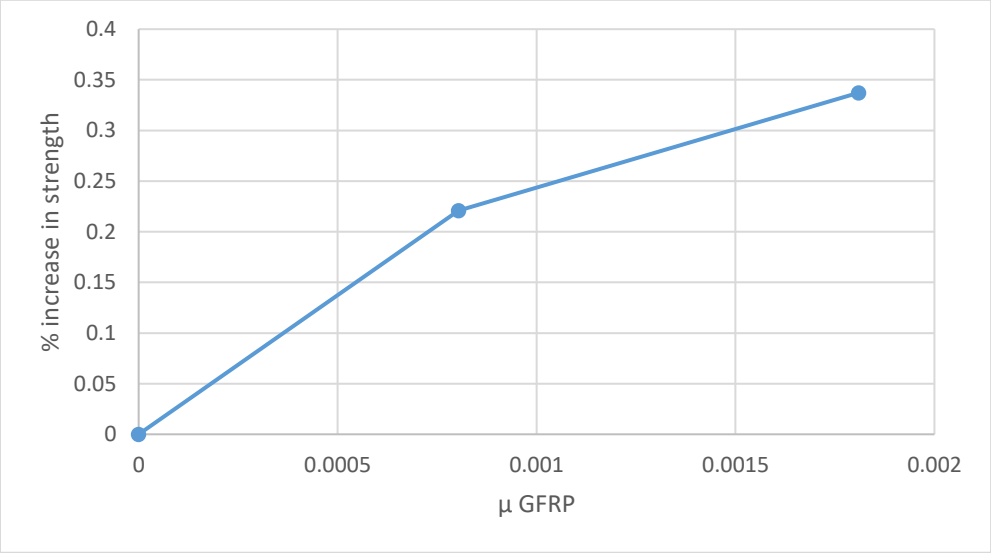

Figure 4.50 (1.5m) Column μ-GFRP vs %Increase in Strength

4.3.1.2 2.0m Column Comparison (effect of GFRP ratio)

Figure 4.51 shows that for the same column height (slenderness) the failure load of the 2.0m column increased from an average of 450 kN for the control sample to an average of 630 kN for the no.8 GFRP strengthened column. This is an increase of 40%. The no. 12 GFRP strengthened column failed at an average load of 600 kN. This is an

increase of 34% compared to the control column and almost the same increase compared to the no.8 GFRP strengthened column. Figure 4.52 shows that the percentage of strength enhancement drops from the μ-GFRP of 0.0008 to μ-GFRP of 0.0018. The results show that the no.8 GFRP bar showed the most increase in strength, which needs to be studied further.

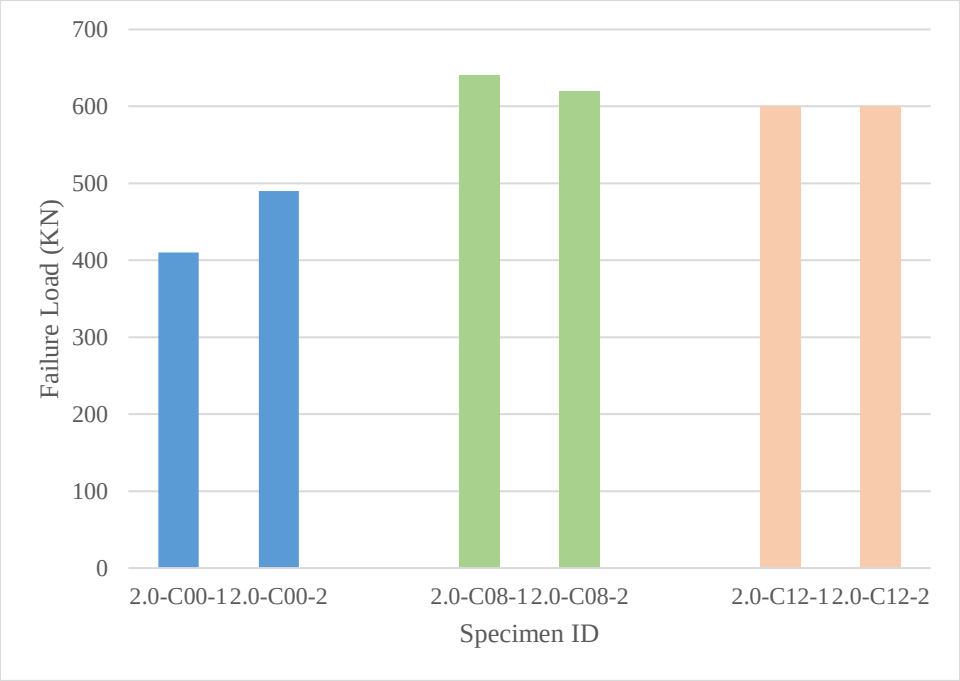

Figure 4.51 (2.0m) Column Failure Load Comparison

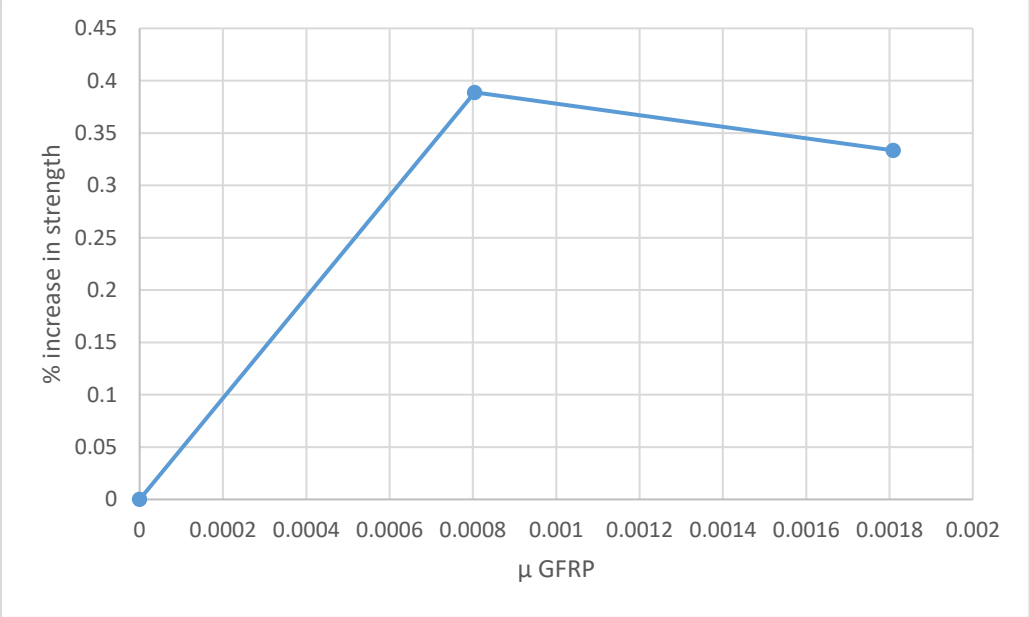

Figure 4.52 (2.0m) Column μ-GFRP vs %Increase in Strength

4.3.1.3 2.5m Column Comparison (effect of GFRP ratio)

Figure 4.53 shows that for the same column height (slenderness) the failure load of the 2.5m column increased from an average of 445 kN for the control sample to an average of 500 kN for the no.8 GFRP strengthened column. This is an increase of 12%. The no. 12 GFRP strengthened column failed at an average load of 580 kN. This is an increase of 31% compared to the control column and 16% compared to the no.8 GFRP strengthened column. Therefore, as seen in Figure 4.54, as the μ-GFRP increases, the percentage of strength enhancement increases.

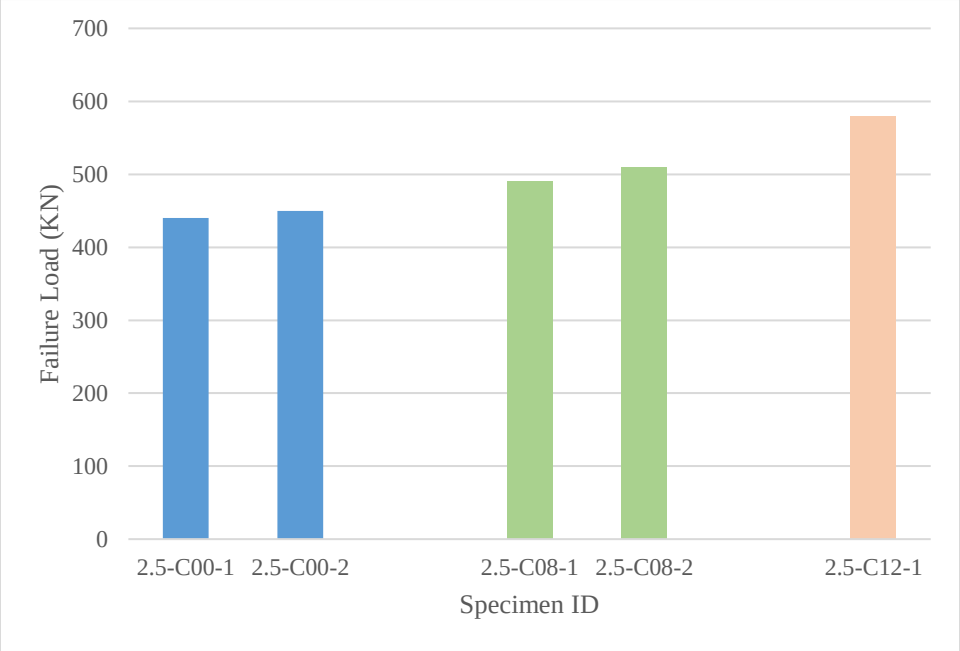

Figure 4.53 (2.5m) Column Failure Load Comparison

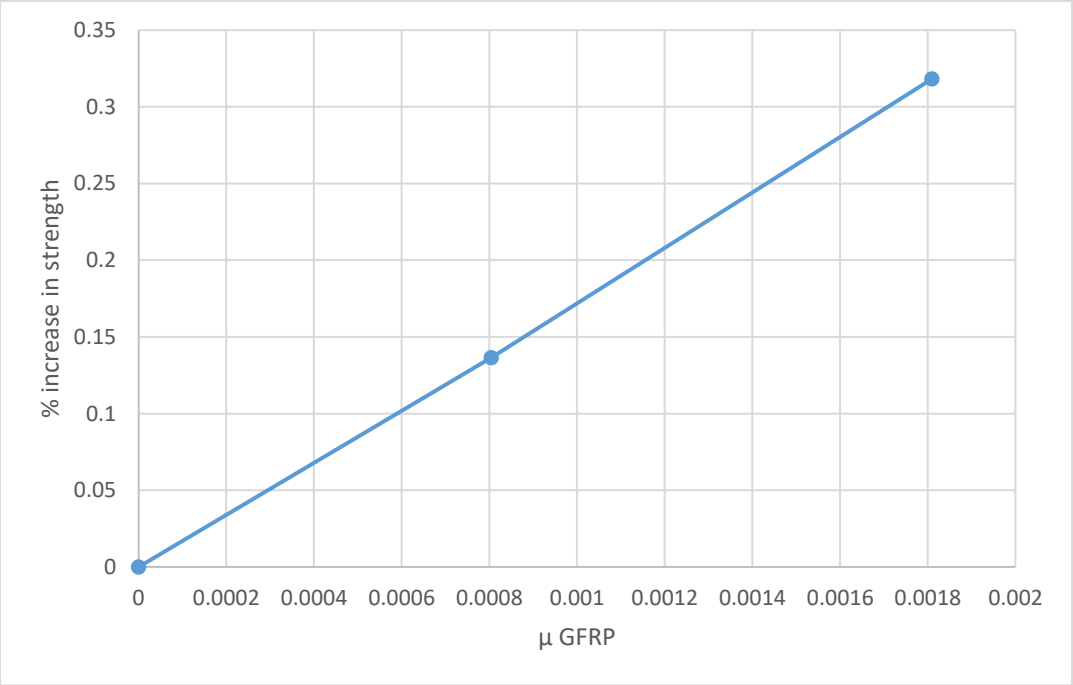

Figure 4.54 (2.5m) Column μ-GFRP vs %Increase in Strength

4.3.2 Effect of Slenderness

4.3.2.1 Control Sample Slenderness Comparison

Figure 4.55 shows that as the column height increases from 1.5m to 2m (hence the slenderness ratio increases from 12 to 16 as shown in Table 3.1), the failure load increased from 430 kN to 450 kN respectively. This is an increase of 5%. The 2.5m column (with a slenderness ratio of 20) has an average failure load of 445 kN. This is a 3.5% increase compared to the 1.5m and a 2% decrease compared to the 2m column. The results show that the 2m column had the highest failure load. This needs to be studied in more depth in future research.

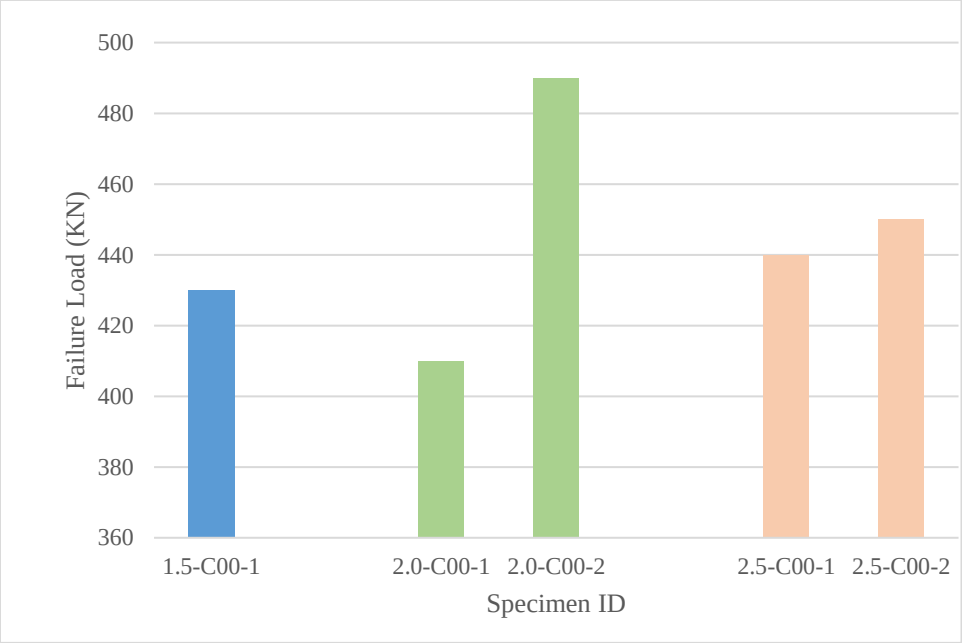

Figure 4.55 Failure Loads Comparison for Control Columns for the Different Column Heights

4.3.2.2 GFRP no.8 Slenderness Comparison

Figure 4.56 shows that as the column height increases from 1.5m to 2m (hence the slenderness ratio increases from 12 to 16 as shown in Table 3.1), the failure load increased from an average of 525 kN to 630 kN respectively. This is an increase of 20%. The 2.5m column (with a slenderness ratio of 20) has an average failure load of 500 kN. This is a 5% decrease compared to the 1.5m and a 21% decrease compared to

the 2m column. Figure 4.57 shows that the percentage strength enhancement increases from 22% at kl/r =12 to a maximum of 39% at kl/r = 39% and then decreased again to 14% at kl/r = 14%. The results show that the 2m column had the highest failure load. This needs to be studied in more depth in future research.

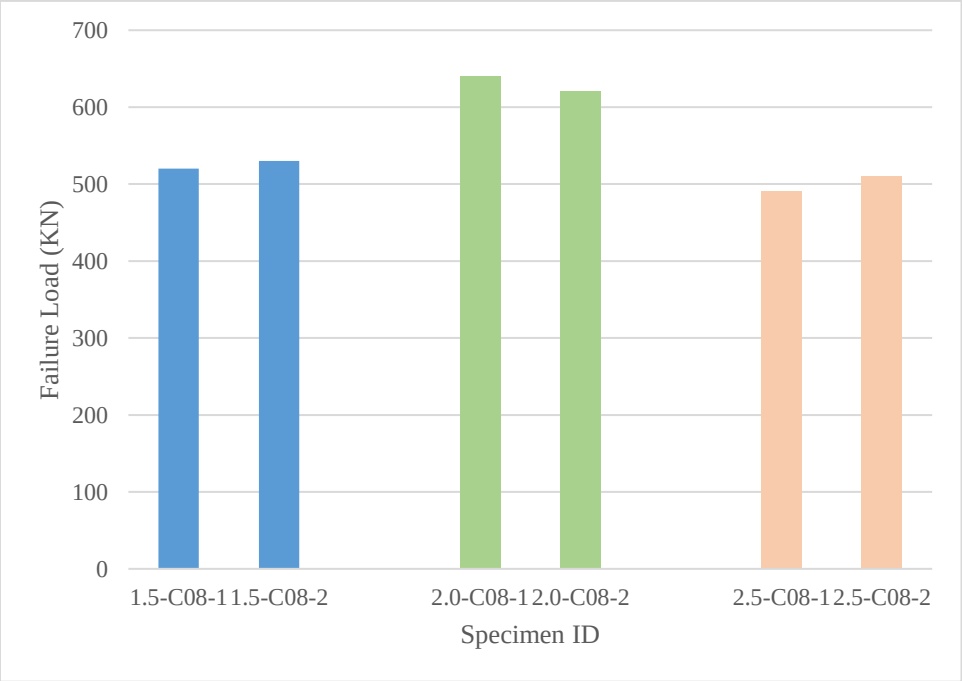

Figure 4.56 Failure Loads Comparison for GFRP no.8 for the Different Column Heights

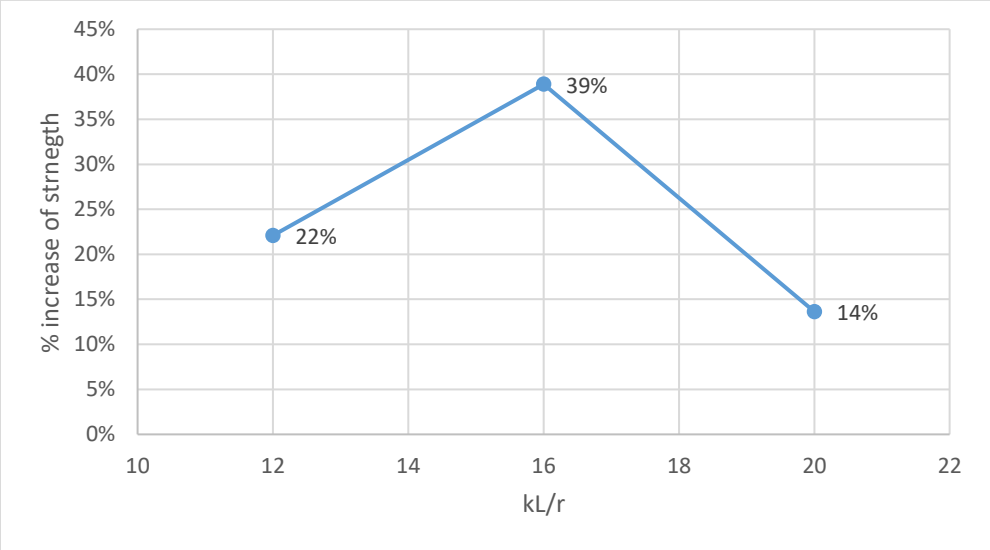

Figure 4.57 Column Slenderness vs % Increase in Strength for μ-GFRP=0.0008

4.3.2.3 GFRP no.12 Slenderness Comparison

Figure 4.58 shows that as the column height increases from 1.5m to 2m (hence the slenderness ratio increases from 12 to 16 as shown in Table 3.1), the failure load increased from an average of 575 kN to 600 kN respectively. This is an increase of 5%. The 2.5m column (with a slenderness ratio of 20) has an average failure load of 580 kN. This is almost like the 1.5m and a 4% decrease compared to the 2m column. Figure 4.59 shows that the percentage of strength enhancement is almost the same for all slenderness ratios. The results show that the 2m column had the highest failure load. This needs to be studied in more depth in future research.

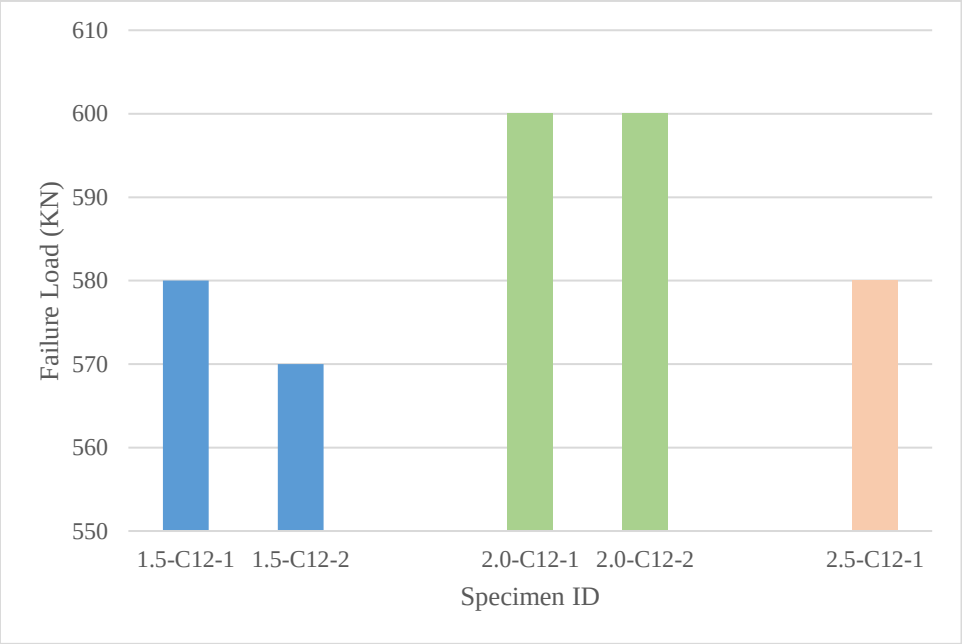

Figure 4.58 Failure Loads Comparison for GFRP no.12 for the Different Column Heights

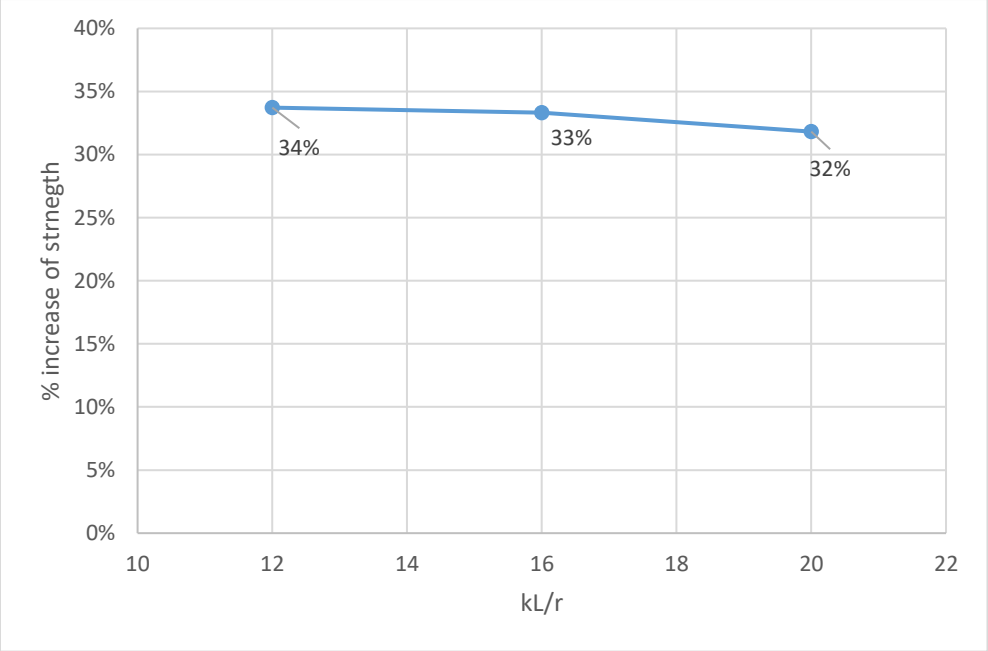

Figure 4.59 Column Slenderness vs % Increase in Strength for μ-GFRP=0.0018

From the slenderness comparison above, the following can be concluded. As the column height increases from 1.5m to 2m, hence increasing the slenderness ratio from 12 to 16, the failure load increases. Then as the height increases to 2.5m (slenderness ratio 20) the failure load decreases again. This can be explained as follows: the increase in column height, hence increase in slenderness means that the column should fail at a lower load. However, this increase in slenderness means that the column will have a greater deformation. Taking this into consideration, the p-delta effect increases. Since the applied load is eccentric, the second order effect means that the column is moving closer to the load and therefore the eccentricity of the load has a lower effect, hence the column bearing more load before failing.

However, this is not the case for the 2.5m column as the slenderness ratio increases to 20, which is the maximum acceptable slenderness ratio according to the ACI. Moreover, the second order effect also increases greatly, hence significantly increasing the moment on the column. Consequently, the column failure load decreases again.

Chapter 5 – Conclusions and Recommendations

The main objectives of this research are to gain a better understanding and to investigate the feasibility and the efficiency of using Near Surface Mounted (NSM) Glass Fibre-Reinforced Polymer (GFRP) bars to enhance the strength of eccentrically loaded reinforced concrete columns. This chapter gives a full summary and conclusions of the work covered by this study, providing recommendations for future research work, as well as concrete applicators.

Chapters one and two gave an introduction on the subject and summarized the experimental data available about near surface mounted FRP bars and laminates for strengthening of concrete structures. They showed that the available test data on using NSM GFRP bars are rare, and that additional tests are required to gain a better understanding of this strengthening technique, and to enable better calibration of future analytical models. The literature review showed that there are no experimental tests on columns strengthened using NSM GFRP bars.

To contribute in this area, seventeen columns were prepared and tested in flexure. The effects of numerous variables on the behavior were studied, including diameter of NSM reinforcement (GFRP bars) and the slenderness ratio (column height).

5.1 Conclusions

From the results obtained through the experimental program, the following main conclusions can be highlighted:

1. The load carrying capacity of eccentrically loaded reinforced concrete columns can be significantly increased using the NSM GFRP bars. The increase in load is 25% for μ_{GFRP} of 0.0008 and by 33% for μ_{GFRP} of 0.0018.
2. There was a 8% increase in carrying capacity from increasing the μ_{GFRP} by 0.1%, this shows that an increase in μ_{GFRP} will increase the column failure load
3. The NSM GFRP strengthening technique allowed the column to experience significantly larger vertical and horizontal deflection and allowed the column to fail in a more ductile manner.

4. The presence of NSM strengthening reinforcement controlled the formation and width of the diagonal cracks and increased the cracking load. This may be attributed to the use of epoxy resin which significantly increase cracking resistance.
5. As the column slenderness increases, the p-δ effect increases. Consequently, the failure load decreases. This is also applicable to the NSM GFRP strengthened columns
6. For the different column heights and GFRP diameters used, all samples' mode of failure was due to flexure.

5.2 Recommendations for Future Work

Since near surface mounted technique is relatively new to the construction industry, it is expected to project further research work to both validate and better understand the feasibility of this technique. The following are a set of recommendations for future research work:

- Upon validation of the results achieved herein, developing design equations for the strengthening of long columns is recommended
- Performing similar work to the one conducted in this study using diverse materials, dimensions and GFRP bars among others
- Conducting finite element in which results are to be compared to experimental work results
- Studying the effect of dynamic loads on NSM GFRP strengthened columns while subjected to other forms of loading

5.3 Recommendations for Concrete Applicators

The results of this study highlight advantages of strengthening of long RC columns using near surface mounted GFRP bars. Hence, the construction industry is urged to consider this relatively innovative technique in future applications using rehabilitation of structure works. It is recommended that Egyptian codes of practice consider provisions in future code revisions to include NSM GFRP, while highlighting advantages and limitations. There is a dire need for the industry to strengthen their

cooperation with both academic societies as well as construction pioneering projects, towards safe and effective methods of NSM GFRP into future applications.

References

ACI Committee 318, “Building Code Requirements for Reinforced Concrete (ACI 318M-05) and Commentary ACI 318 R-05,” American Concrete Institute, Detroit, 2005, 436 PP.

ACI 440R-96, “State of the Art Report on Fibre Reinforced Plastic (FRP) Reinforcement for Concrete Structures”, American Concrete Institute, Detroit, 1996, 65 pp.

ACI Committee 318, 1970. “Building Code Requirements for Reinforced Concrete (ACI 318M-1970).

Blaszak, G. and Gold, W., "Strengthening structures with FRP Systems," Conference on Seismic Repair and Rehabilitation of Structures, Fullerton, California, March 21-22, 2000, pp.10-19.

Catbas, K. H.."Performance of Beams Eternally Reinforced with Carbon Fibre Reinforced Plastic Laminates," Masters Thesis, Department of Civil and Environmental Engineering, University of Cincinnati, 1997, pp.92

Coelho, Sena-Cruz and Neves, "A review on the bond behavior of FRP NSM systems in concrete" Construction and Building Materials Journal, 2015.

De Lorenzis, L, "Anchorage Length of Near-Surface Mounted Fibre-Reinforced Polymer Rods and Concrete in Structural Strengthening-Analytical Modeling", ACI Structural Journal, V. 101, No. 3, 2004, pp. 375-386.

De Lorenzis, L. and Nanni, A.,"Bond Between Near-Surface Mounted Fibre-Reinforced Polymer Rods and Concrete in Structural Strengthening", ACI Structural Journal, V. 99, No. 2, 2002, pp. 123-132.

De Lorenzis, L. and Nanni, A., "Shear Strengthening of Reinforced Concrete Beams with Near-Surface Mounted Fibre-Reinforced Polymer Rods", ACI Structural Journal, V. 98, No. 1, Jan.-Feb., 2001, pp. 60-68.

De Lorenzis, L., "Strengthening of RC Structures with Near-Surface Mounted FRP Rods", MSc Thesis, Department of Civil Engineering, University of Missouri – Rolla, rolla, MO, 2000, pp. 175.

Ehsani, M. R., Saadatmanesh, H., and Tao, S., "Bond of GFRP Rebars to Ordinary-Strength Concrete," Fibre-Reinforced-plastic Reinforcement for Concrete Structures, SP-138, American Concrete Institute, Detroit, 1993, pp. 333-345.

Faza, S., and GangaRao, H. V. S., "Bending Response of Beams Reinforced with FRP Rebars for Varying Concrete Strength," Advanced Composite Materials in Civil Engineering Structures, ASCE New York, 1991, pp. 262-270.

Franke, L. "Behavior and Design of High-Quality Glass-Fibre Composite Rods as Reinforcement for Prestressed Concrete Members," Report, International Symposium, CP/Ricem/I BK, Prague, 1981, 52 pp.

Hassan, T.K. and Rizkalla, S., "Bond Mechanism of Near-Surface-Mounted Fibre-Reinforced Polymer Bars for Flexural Strengthening of Concrete Structures," ACI Structural Journal, V. 101, No. 6, 2004, pp. 830-839.

Kheyroddin, A. and Kargaran, A., "Experimental and Numerical Investigation of Seismic Retrofitting of RC Square Short Columns Using FRP Composites," Structural Concrete Journal of the fib, 2019.

Porter, M. L., Hughes, B. W., Barnes, B. A., and Vis-wanath, K. P., "Non-Corrosive Tie Reinforcing and Dowel Bars for Highway Pavement Slabs," Department of Civil and Construction Engineering Research Institute, Iowa State University, Ames. 1993.

Rahai, A. and Akbarpour, H., "Experimental study on the effect of CFRP strengthening on high slender RC columns subjected to cyclic axial compression load and biaxial bending," 2017

Rubinsky, I.A. and Rubinsky, A., "An Investigation into the Use of Fibre-Glass or Prestressed Concrete," Magazine of Concrete Research, V.8. 1954.

Shehata, E., Morphy, R. and Rizkalla, S., "Fibre Reinforced Polymer Shear Reinforcement for Concrete Members: Behavior and Design Guidelines," Canadian Journal of Civil Engineering, V. 27, 2000, pp. 859-872.

Schwarz, M. M., Composite materials handbook, McGraw-Hill, Inc., New York. 1992

Schoeck ComBAR Brochure and Properties. August 2018.

Si Youcef, Y., Amziane, S. and Chemrouk, M., "CFRP confinement effectiveness on the behavior of reinforced concrete columns with respect to buckling instability," Construction and Building Materials, vol. 81, p. 81–92, 2015.

Yan, X., Miller, B., Nanni, A., and Bakis, C.E., Characterization of CFRP Rods Used as Near Surface Mounted Reinforcement," Proceedings of the 8th International Structural Faults and Repair Conference, M.C. Forde, Ed., Engineering Technics Press, Edinburgh, Scotland, 1999, 10 pp.